

Development of a Multiphase Incompressible flow Solver

Vishwas Rana Salvaji

A Dissertation Submitted to
Indian Institute of Technology Hyderabad
In Partial Fulfillment of the Requirements for
The Degree of Master of Technology

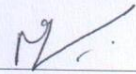


Department of Mechanical & Aerospace Engineering

July 2015

Declaration

I declare that this written submission represents my ideas in my own words, and where ideas or words of others have been included, I have adequately cited and referenced the original sources. I also declare that I have adhered to all principles of academic honesty and integrity and have not misrepresented or fabricated or falsified any idea/data/fact/source in my submission. I understand that any violation of the above will be a cause for disciplinary action by the Institute and can also evoke penal action from the sources that have thus not been properly cited, or from whom proper permission has not been taken when needed.



(Signature)

(Vishwas Rana Salvaji)

(ME13M1035)

Approval Sheet

This Thesis entitled Development of a Multiphase Incompressible flow Solver by Vishwas Rana Salvaji is approved for the degree of Master of Technology from IIT Hyderabad



(Dr. Mangadoddy Narasimha) Examiner
Dept. of Chemical Engineering
IITH



(Dr. Harish Nagaraj Dixit) Examiner
Dept. of Mechanical & Aerospace Engineering
IITH



(Dr. Raja Banerjee) Adviser
Dept. of Mechanical & Aerospace Engineering
IITH

Acknowledgements

I would like to express my gratitude to my guide Dr. Raja Banerjee for his guidance and helping me with valuable inputs in project. I would especially like to thank him for his moral support and calmness, at the time when I have been running on low confidence with the project work. His honesty and humility, has always motivated us to work harder and has kept us grounded. And simultaneously, he has been the source of motivation for all our friends. Thus, the work environment, I have got to work has been vibrant and energetic.

I would like to thank Dr. M.Narsimha and Dr. K.Venkatasubbaiah for the time and support they given me in understanding the Mixture model. I would like to thank Vatsalya Sharma for his valuable suggestion at various point of the Project. In addition, he has helped us in understanding the *Thunder strom* solver, which has been the starting point for this thesis. I would also like to thank all my friends who have always maintained an atmosphere of co-operation and friendship. Thus, have made my memorable experience.

I would like to thank my guide and the entire IIT Hyderabad system for providing us an excellent computational facility to work upon.

At last I would like thank my parents for their support, that built my confidence in achieving my goals.

Abstract

Mixture Model is least computational approach for solving Multiphase problems. We aim to develop a general-purpose and robust incompressible flow solver to help in analysing Jets for laminar flows. The present work aims to include Mixture Model in Thunder Strom Solver developed by previous post-graduate student. In this work, disperse phase is considered as solid particals and a Lagrangian algebraic slip mixture model has been deployed to study gas-particle two phase flows. By the above approach the relation between Euler and Lagrangian equations is established. Results of differetnt density ratios and loadings are validated by comparing with commercial solver Fluent.

Contents

Declaration	ii
Approval Sheet	iii
Acknowledgements	iv
Abstract	v
1 Introduction	1
1.1 Literature survey	3
1.2 Objective of present work	4
2 Governing Equations of Mixture Model	5
2.1 Field Equations	6
2.1.1 Continuity equation of mixture	7
2.1.2 Momentum equation of mixture	7
2.1.3 Continuity equation of phase	9
2.1.4 Relative velocity	10
2.1.5 Relaxation Time τ_p	12
2.1.6 Drag Force	12
2.2 Constitutive Equations	13
2.3 summary	16
3 Discretization of Equations	18
3.1 Solution algorithm	18
3.1.1 SemiImplicit Algorithm	19
3.2 Closure	22
4 Laminar Validation of Multiphase Module	23
4.1 Introduction	23
4.2 Different Density Ratios	24
4.2.1 Density ratio 1.1	24
4.2.2 Density ratio 10:	30
4.2.3 Density ratio 100	33
4.3 Closure	36

5 Results and Discussion	37
5.1 Grid Independence	37
5.2 Comparison of different Drag models	42
6 Conclusion and Future work	49
Appendices	50
A Source Terms Formulation	51
References	53

Chapter 1

Introduction

To develop a multiphase solver which is used to solve computational flows for engineering problems, significantly in Jets. Unstructured grids are used for grid generation because lesser computational cost and their ease in adapting the complex domain, when compared to structured grids. Most of the engineering problems involve turbulent flow through complex flow domains. Major of current work is done in laminar flow and will be extended to Turbulent flows .

Jet systems are widely used in many chemical, petrochemical and biochemical industries, such as absorption, oxidation, coal combustion, food and commodity transfer, solid rocket jets, pharmaceutical granulators , coal liquefaction, coal combustion boilers and aerobic fermentation. When a Jet from the nozzle, it causes a turbulent stream to enable an optimum interaction between the phases. Because of low cost and ease of maintenance, it is built in numerous forms of construction. The mixing is done by the droplets and it requires less energy. In thesis we mainly concentrate on solving the problems in gas-solid particle two-phase flow using Lagrangian algebraic slip mixture model(LASMM). In two-phase flow, we consider dispersed phase as solid particles which is considered to be fine powder with size is from micrometers to several hundred micrometers. The flow is considered to be homogeneous and interfacial forces between the particles like drag force, lift force, virtual mass force etc is included by employing Lagrangian Algebraic Slip Mixture Model(LASMM). By this accuracy of Mixture Model is increased.

A Multiphase system is defined as a mixture of the phases of solid, liquid and gases. Multiphase flows are often classified according to the nature of the system [1]: dispersed flows like particle or droplet in liquid or gas, bubbles in liquid, Separated flows like annular flows in circular pipes, stratified flow in horizontal pipes, and Transitional flows combination of both the flows. Depending on the strength of the coupling between the phases, different modeling approaches are suggested. In the Euler-Euler approach, the different phases are treated mathematically as inter penetrating continuum. Since the volume of a phase cannot be occupied by the other phases, the concept of phase volume fraction is introduced. These volume fractions are assumed to be continuous functions of space and time and their

sum is equal to one. Conservative equations for each phase are derived to obtain a set of equations, which have similar structure for all phases. These equations are closed by providing constitutive relations that are obtained from empirical information. The different Euler-Euler approach are given below.

The VOF Model: The VOF (Volume of Fluid) Model is a surface-tracking technique applied to a fixed Eulerian mesh. It is designed for two or more immiscible fluids where the position of the interface between the fluids is of interest. In the VOF model, a single set of momentum equations is shared by the fluids, and the volume fraction of each of the fluids in each computational cell is tracked throughout the domain. Applications of the VOF model include stratified flows, free-surface flows, filling, sloshing, the motion of large bubbles in a liquid, the motion of liquid after a dam break, the prediction of jet breakup (surface tension), and the steady or transient tracking of any liquid-gas interface.

The Mixture Model: The Mixture model is a simplified multiphase model that can be used to model multiphase flows where the phases move at different velocities, but assume local equilibrium over short spatial length scales. The mixture model solves for the mixture momentum equation and have algebraic expressions for the relative velocities between the phases. Applications of the mixture model include particle-laden flows with low loading, bubbly flows, sedimentation, and cyclone separators. The mixture model can also be used without relative velocities for the dispersed phases to model homogeneous multiphase flow.

The Eulerian Model: The Eulerian model is the most complex of the multiphase models. It solves a set of momentum and continuity equations for each phase. Coupling between the phases is achieved through the pressure and inter-phase exchange coefficients. Applications of the Eulerian multiphase model include bubble columns, risers, particle suspension, and fluidized beds.

From the above discussion we can say that the Mixture model and the Eulerian model are ease to implement for solving multiphase flows. The Mixture model and the Eulerian model are appropriate for flows in which the phases mix or dispersed-phase volume fractions exceed 10%. The main reason behind choosing Mixture model over Eulerian Model is computational effort. If there is a wide distribution of the dispersed phases the mixture model is preferable due to computational effort but the accuracy of Mixture Model is less than Eulerian Model. And also complexity of the Eulerian model can make it less computationally stable than the mixture model. Accuracy of Mixture Model can be improved by using Lagrangian algebraic slip velocity approach (slip velocity concept) which is discussed in chapter 2. In this model the slip velocity between gas and solid particles was derived from Lagrangian form. Hence the accelerations of various forces on the particle were considered

through the single solid particle Lagrangian momentum equation. Owing to the governing equations of LASMM based on Euler equations, this model therefore realized the connection between Eulerian model and Lagrangian model. Through the comparisons of the numerical simulations of code to fluent, this model was validated for laminar flows.

Finite Volume method has been used for discretization of governing equations. The method of discretization for unstructured grid is discussed in thesis of Vatsalya Sharma [2]. In the Finite Volume method, the solution domain is subdivided into a number of finite volume cells defined by the coordinates of their vertices read from the CGNS grid. Collocated grid arrangement has been implemented where all the dependent variables are defined at the centroid of the individual cells. Primitive variables (like velocity and temperature) are being solved directly.

1.1 Literature survey

The report on Mixture Model by Mikko Manninen and Veikko Taivassalo [3] deals with two-phase gas-particle flow, explains about the effect of different drag models and closure equations of slip(relative) velocity. The form of the constitutive equations for the relative velocities varies in the different mixture model. The basic assumption in this formulation is that a local equilibrium establishes over short spatial length scales. A group of models have been developed on the basis of assumptions of a local equilibrium and depending upon exact formulations used to determine the velocity differences model is called as drift flux model[4], the mixture model[1], Algebraic slip model[5], the suspension model[6], the diffusion flux model[7][1],local equilibrium model[8]. In addition, the closure relations for multiphase flow include uncertainties [9] [10] which were ignored to make the equations simpler. Different constitutive relations have been examined [11] for the determination of relative velocity. The Drag force represents additional forces on a particle due to velocity relative to the fluid. Different formulations of drag coefficient are studied [12] [13][14]. Many assumptions are made to keep computation of gas-particle flow simpler but in dense suspensions, particle tend to form clusters affecting the average drag force[15].

There are many applications of Mixture model in industrial problems. The separation of a solid particles in a liquid due to gravitation and centrifugal forces is extensively studied using mixture model[16][17]. One of the major application of this model is in hydrocyclone problems. Pericleous & Drake [5] modeled the flow of the air, liquid and particles in a complicated hydro cyclone classifier by using mixture model. Brennan [18] used Mixture model for hydro cyclone problems with different Turbulent model and found that LES simulations gave good agreement with experimental data . By Lagrangian particle method, M.Narsimha [19] were able to simulate dense medium cyclone which was modeled by coupling components models for the air core, the magnetite medium and coal particles. The results showed good agreement with experimental data. The gas-solid two phase flow is mainly seen in

powder technology, Zhi Shang [20] has validated mixture model with the experimental data in gas-solid two phase flows. Algebraic slip Mixture model of gas-particle flows generally used for simulation of wind blown particles like sand, snow. Alhajraf [21] used the model to simulate the flow field around fences for two applications, snow drift at single row fence and sand drift at double row fence. Akbarinia [22] has used mixture model on laminar mixed convection heat transfer in a circular Curved tube with a nanofluid consisting of water and 0.01 volume of Aluminum oxide, to investigate effects of the diameter of particles on the hydrodynamic and thermal parameters. The drift flux model has been implemented by Ruichang [23] for the analysis of two dimensional two phase flow in horizontal heated tube bundles. The present work relies on the unstructured grid handling schemes proposed by Dr. Dalal [24]. The discretization of equations according to unstructured grid is taken from the thesis of Vatsalya sharma [2].

1.2 Objective of present work

- To develop robust Multiphase module in Thunderstorm solver by incorporating Lagrangian Algebraic Slip Mixture Model (LASMM) .
- To incorporate different Drag Models.
- To validate this solver for different density ratios with different loading for the 3D cases for laminar flow.

Chapter 2

Governing Equations of Mixture Model

A multiphase flow system consists of a number of single phase regions bounded by moving interfaces. The description is limited to dispersed multiphase flows. The theory of gas particle system contains several complications i.e, the size distribution, other physical properties of the solid particles and the collision processes of the solid particles with each other and with gas molecules are difficult to account for. The theory for the application of Mixture model on gas-solid particle two-phase flow taken from the report of Mikko Manninen and Veikko Taivassalo [3].

The Lagrangian approach treats the fluid phase a continuum and the time average is taken by following a certain solid particles and observing it at some time level. Particle trajectories are calculated from the equation of particle motion. Lagrangian averages are popular especially in modeling the dynamics of single particle or dilute suspension and been extended to more dense flows[25].

In the Eulerian approach, the particle phase is also treated as continuum. It consists of three essential parts: Field equations consists of conservative principles momentum and mass, Constitutive equation close the equation system by taking into account the structure of the flow and material properties by experimental correlations.

The averaged equations of multiphase flow can be written in numerous ways. Equations can be derived by time averaging, space averaging, or by combination of these. In all these methods the resulting equation contain basically same terms. Modeling of the turbulent terms is essential part of the equation closure . The field equations are given below in general form and later used for deriving the basic equations for mixture model. We restrict our analysis on the mechanics of multiphase system. Therefore thermodynamic relations are not considered.

If we denote the local instant velocity of the phase k by \mathbf{u}_{Ik} , the averaged velocity can be defined as $\mathbf{u}_k = \overline{u_{Ik}}$, where over bar indicates the averaging domain .The alternative

definition of the averaged velocity is based on weighing the velocity with the local density ρ_k

$$\mathbf{u}_k = \frac{\overline{\rho_{Ik}\mathbf{u}_{Ik}}}{\overline{\rho_{Ik}}} = \frac{\overline{\rho_{Ik}\mathbf{u}_{Ik}}}{\rho_k} \quad (2.1)$$

ρ_k denotes the average material density, \mathbf{u}_k denotes Favre averaged velocity.

The Favre averaged balance equations are presented by several authors [1][13][26]. We follow notations of Mikko Manninen and Veikko Taivassalo [3]. According to it the continuity and momentum equations for each phase k as follows

$$\frac{\partial}{\partial t}(\phi_k \rho_k) + \nabla \cdot (\phi_k \rho_k \mathbf{u}_k) = \Gamma_k \quad (2.2)$$

$$\begin{aligned} \frac{\partial}{\partial t}(\phi_k \rho_k \mathbf{u}_k) + \nabla \cdot (\phi_k \rho_k \mathbf{u}_k \mathbf{u}_k) = & -\phi_k \nabla p_k + \phi_k \rho_k g \\ & + \nabla \cdot [\alpha_k (\boldsymbol{\tau}_k + \boldsymbol{\tau}_{Tk})] + M_k \end{aligned} \quad (2.3)$$

where ϕ_k is the volume fraction of phase k . The term Γ_k represents the rate of mass generation of phase k at the interface and M_k is the average inter-facial momentum source for the phase k , $\boldsymbol{\tau}_k$ and $\boldsymbol{\tau}_{Tk}$ are the average stress tensor and turbulent stress tensor.

$$\boldsymbol{\tau}_{Tk} = -\overline{\rho_{Ik}\mathbf{u}_{Fk}\mathbf{u}_{Fk}} \quad (2.4)$$

\mathbf{u}_{Fk} is the fluctuating component of the velocity, i.e. $\mathbf{u}_{Fk} = \mathbf{u}_{Ik} - \mathbf{u}_k$. Before they are solved constitutive equations for the average stress, turbulent stress term and the inter-facial forces between the phases have to be formulated. As current work deals with the laminar flow, Turbulent stress terms are neglected in all the equations.

A common simplification that we discussed earlier in multiphase flows is that the dispersed phase is assumed to be consisting of spherical particles of a single average particle size. The interactions between different phases are frequently neglected. A typical assumption is that the particles are distributed in a homogeneous way inside the local averaged domain corresponding to the control volume.

2.1 Field Equations

Consider a mixture with n phases. Assume one phase is continuous phase with a subscript c . The dispersed phases can comprise of particles. In this approach both continuity and momentum equations are written for the mixture of phases. The particle concentrations are solved from continuity equations of each discrete phase. The momentum equations for each discrete phase are approximated by algebraic equations. The mixture model equations are derived in the literature applying various approaches [26][1][7]. In this we derive general equations of mixture model starting from equations of individual phases.

2.1.1 Continuity equation of mixture

From the continuity equation (2.2) by summing over all the phases.

$$\frac{\partial}{\partial t} \sum_{k=1}^n (\phi_k \rho_k) + \nabla \cdot \sum_{k=1}^n (\phi_k \rho_k \mathbf{u}_k) = \sum_{k=1}^n \Gamma_k \quad (2.5)$$

As total mass is conserved, mass generation term must be zero.

$$\sum_{k=1}^n \Gamma_k = 0 \quad (2.6)$$

We obtain the continuity equation of the mixture

$$\frac{\partial \rho_m}{\partial t} + \nabla \cdot (\rho_m \mathbf{u}_m) = 0 \quad (2.7)$$

Here the mixture density and mixture velocity are defined as

$$\rho_m = \sum_{k=1}^n \phi_k \rho_k \quad (2.8)$$

$$\mathbf{u}_m = \frac{1}{\rho_m} \sum_{k=1}^n (\phi_k \rho_k \mathbf{u}_k) \quad (2.9)$$

\mathbf{u}_m represents the velocity of mass center. Note that ρ_m varies but the material densities will be constant.

2.1.2 Momentum equation of mixture

The momentum equation for mixture as follows from(2.3) by summing over all phases

$$\begin{aligned} \frac{\partial}{\partial t} \sum_{k=1}^n (\phi_k \rho_k \mathbf{u}_k) + \nabla \cdot \sum_{k=1}^n (\phi_k \rho_k \mathbf{u}_k \mathbf{u}_k) = & - \sum_{k=1}^n \phi_k \nabla p_k + \sum_{k=1}^n \phi_k \rho_k g \\ & + \nabla \cdot \sum_{k=1}^n \phi_k (\boldsymbol{\tau}_k + \boldsymbol{\tau}_{Tk}) + \sum_{k=1}^n M_k \end{aligned} \quad (2.10)$$

By the definitions of mixture density ρ_m and the mixture velocity \mathbf{u}_m , the second term can be written as

$$\nabla \cdot \sum_{k=1}^n (\phi_k \rho_k \mathbf{u}_k \mathbf{u}_k) = \nabla \cdot (\rho_m \mathbf{u}_m \mathbf{u}_m) + \nabla \cdot \sum_{k=1}^n (\phi_k \rho_k \mathbf{u}_{Mk} \mathbf{u}_{Mk}) \quad (2.11)$$

where \mathbf{u}_{Mk} is the diffusion velocity, i.e., the velocity of phase k relative to the center of the mixture mass.

$$\mathbf{u}_{Mk} = \mathbf{u}_k - \mathbf{u}_m \quad (2.12)$$

The momentum equation of mixture takes the form

$$\begin{aligned} \frac{\partial}{\partial t} (\rho_m \mathbf{u}_m) + \nabla \cdot (\rho_m \mathbf{u}_m \mathbf{u}_m) = \nabla p_m + \nabla \cdot (\boldsymbol{\tau}_m + \boldsymbol{\tau}_{Tm}) + \nabla \cdot \boldsymbol{\tau}_{Dm} \\ + \rho_m g + M_m \end{aligned} \quad (2.13)$$

As flow is laminar, Turbulent stresses in the equation are neglected. The three stresses tensors are defined as

$$\boldsymbol{\tau}_m = \sum_{k=1}^n \phi_k \boldsymbol{\tau}_k \quad (2.14)$$

$$\boldsymbol{\tau}_{Dm} = - \sum_{k=1}^n \phi_k \rho_k \mathbf{u}_{Mk} \mathbf{u}_{Mk} \quad (2.15)$$

The mixture pressure is defined by the relation

$$\nabla p_m = \sum_{k=1}^n \phi_k \nabla p_k \quad (2.16)$$

We consider the phase pressures are often equal i.e, $p_k = p_m$, except in the case of expanding bubble. The last term on right hand side of equation (2.13) is the influence of surface tension force on the mixture and is defined as

$$M_m = \sum_{k=1}^n M_k \quad (2.17)$$

The term M_m depends on the geometry of the interface. The additional term of (2.13) $\nabla \cdot \boldsymbol{\tau}_{Dm}$ represents the momentum diffusion due to relative velocity motion. The Mixture model will

be inaccurate if the above term is missing [6].

2.1.3 Continuity equation of phase

Taking continuity equation of phase (2.2) and applying diffusion velocity (2.12) definition phase velocities are eliminated. The equation we get is:

$$\frac{\partial}{\partial t}(\phi_k \rho_k) + \nabla \cdot (\phi_k \rho_k \mathbf{u}_k) = \Gamma_k - \nabla \cdot (\phi_k \rho_k \mathbf{u}_{Mk}) \quad (2.18)$$

If the phase densities are constant and phase changes do not occur, the continuity equation reduces to

$$\frac{\partial}{\partial t}(\phi_k) + \nabla \cdot (\phi_k \mathbf{u}_k) = -\nabla \cdot (\phi_k \mathbf{u}_{Mk}) \quad (2.19)$$

Above equation referred as diffusion equation [7], accordingly mixture model is often called as diffusion model. In practice the diffusion velocity has to be determined by the relative (slip) velocity which is defined as the velocity of the dispersed phase relative to the continuous phase.

$$\mathbf{u}_{Ck} = \mathbf{u}_k - \mathbf{u}_c \quad (2.20)$$

In two-phase gas-solid particle flow, solid particles often considered as dispersed phase and indicated with the subscript of p . The diffusion velocity of a dispersed phase p , $\mathbf{u}_{Mp} = \mathbf{u}_p - \mathbf{u}_m$, can be presented in terms of relative velocities

$$\mathbf{u}_{Mp} = \mathbf{u}_{Cp} - \sum_{k=1}^n C_k \mathbf{u}_{Ck} \quad (2.21)$$

As we consider only one dispersed phase, above equation take the following form

$$\mathbf{u}_{Mp} = (1 - C_p) \mathbf{u}_{Cp} \quad (2.22)$$

The field equations of mixture model as well as the continuity equation of phase k in terms of mixture velocity were obtained from the original phase equations by algebraic manipulations. The closure of field equations require as in full multiphase models. The most important assumption of the mixture model will be made in replacing the phase momentum equations with algebraic equations for the diffusion velocity \mathbf{u}_{Mk} .

2.1.4 Relative velocity

Before solving the continuity equation for phase k and the momentum equation for the mixture, the diffusion velocity has to be determined. In the present analysis we make local equilibrium approximation in the momentum equation for the dispersed phases. In this we consider that particle is accelerated to terminal velocity in short distance. The relative velocity \mathbf{u}_{Cp} often called as slip velocity [5][8] is obtained from force balance equation and is used to calculate diffusion velocity (2.12).

Using the continuity equation (2.2) the momentum equation of dispersed phase d can be written as (turbulent fluctuations are ignored)

$$\begin{aligned} \phi_d \rho_d \frac{\partial \mathbf{u}_d}{\partial t} + \phi_d \rho_d (\mathbf{u}_d \cdot \nabla) \mathbf{u}_d = & -\phi_d \nabla p_d + \phi_d \rho_d g \\ & + \nabla \cdot [\alpha_d \boldsymbol{\tau}_d] + M_d \end{aligned} \quad (2.23)$$

And the corresponding mixture momentum equation after using mixture continuity equation (2.7) is

$$\begin{aligned} \rho_m \frac{\partial \mathbf{u}_m}{\partial t} + \rho_m (\mathbf{u}_m \cdot \nabla) \mathbf{u}_m = & \nabla p_m + \nabla \cdot \boldsymbol{\tau}_m + \nabla \cdot \boldsymbol{\tau}_{Dm} \\ & + \rho_m g + M_m \end{aligned} \quad (2.24)$$

Here in solid particle flow, the surface tension forces are neglected and consequently $M_m = 0$.

We make the assumption that the phase pressures are equal.

$$p_d = p_m = p \quad (2.25)$$

Now eliminate the pressure gradients from two equations by multiplying (2.24) with ϕ_d and subtracting from (2.23). We get the following equation

$$\begin{aligned} M_d = \phi_d \left[\rho_d \frac{\partial \mathbf{u}_{Md}}{\partial t} + (\rho_d - \rho_m) \frac{\partial \mathbf{u}_m}{\partial t} \right] + \phi_d \left[\rho_d (\mathbf{u}_d \cdot \nabla) \mathbf{u}_d - \rho_m (\mathbf{u}_m \cdot \nabla) \mathbf{u}_m \right] \\ - \phi_d (\rho_d - \rho_m) g - \nabla \cdot [\phi_d \boldsymbol{\tau}_d] + \phi_d \nabla \cdot [\boldsymbol{\tau}_m + \boldsymbol{\tau}_{Dm}] \end{aligned} \quad (2.26)$$

Now we will make several approximations to simplify (2.26). Using local equilibrium approximation, we drop the first term the time derivative of \mathbf{u}_{Md} . In the second term, we approximate

$$(\mathbf{u}_d \cdot \nabla) \mathbf{u}_d \approx (\mathbf{u}_m \cdot \nabla) \mathbf{u}_m \quad (2.27)$$

The viscous and diffusion stresses are omitted as small compared to the leading terms. The Turbulent stress is ignored in present work.

In this derivation we are considering only viscous drag. The drag induced momentum transfer M_d is

$$M_d = -\beta \mathbf{u}_{Cd} + M'_d \quad (2.28)$$

where M'_d is the term caused by velocity fluctuations [27]. The drag function β depends on the particle Reynolds number, solid concentration and particle size. Many models are available for β formulation. For the derivation we take the model of Ishii & Mishima [13], then β takes the form

$$\beta = \frac{3}{4} C_D \frac{\phi_d \rho_c |\mathbf{u}_{Cd}|}{d_d} \quad (2.29)$$

where C_D is determined by drag models. From the equations (2.26) we get the final simplified equilibrium equation for the relative velocity

$$\frac{1}{2} \rho_c A_d C_D |\mathbf{u}_{Cd}| \mathbf{u}_{Cd} = V_d (\rho_d - \rho_m) \left[g - (\mathbf{u}_m \cdot \nabla) \mathbf{u}_m - \frac{\partial \mathbf{u}_m}{\partial t} \right] + M'_p \quad (2.30)$$

Generally the relative velocity have fluctuations [1]. But for simplification fluctuations are neglected. Therefore the equation (2.30) takes the following form

$$\frac{1}{2} \rho_c A_d C_D |\mathbf{u}_{Cd}| \mathbf{u}_{Cd} = V_d (\rho_d - \rho_m) \left[g - (\mathbf{u}_m \cdot \nabla) \mathbf{u}_m - \frac{\partial \mathbf{u}_m}{\partial t} \right] \quad (2.31)$$

The generalized equation for the slip velocity

$$\mathbf{u}_{Cd} = \frac{\tau_d}{f_{drag}} \frac{(\rho_d - \rho_m)}{\rho_d} \left[g - (\mathbf{u}_m \cdot \nabla) \mathbf{u}_m - \frac{\partial \mathbf{u}_m}{\partial t} \right] \quad (2.32)$$

where τ_d is relaxation time, f_{drag} drag function.

The simplest algebraic slip formulation is the so-called drift flux model, in which the acceleration of the particle is given by gravity and/or a centrifugal force and the particulate relaxation time is modified to take into account the presence of other particles.

2.1.5 Relaxation Time τ_p

The particle relaxation time is a measure of particle inertia and denotes the time scale with which any slip velocity between the particles and the fluid is equilibrated [28]. The local equilibrium approximation requires that the particle is rapidly accelerated to the terminal velocity. A criteria for neglecting the acceleration is related to the relaxation time of the particle, τ_p defined by simplified equations. τ_d is given by

$$t_d = \frac{\rho_d d_d^2}{18\mu_m} \quad (2.33)$$

We assume that the suspension is homogeneous in small spacial scales. If this is not the case and the dense clusters of particles are formed, the mixture model usually not applicable. The clustering can lead to a substantial decrease in the effective drag coefficient and the local equilibrium approximation is not valid. Although the mixture model principle valid for small particles ($d_d < 50\mu m$), it can be used only for dilute suspension with secondary to primary phase mass ratio below 1.

2.1.6 Drag Force

The Drag force represents the additional forces on a particle due to velocity relative to fluid. For a single rigid spherical particle in a fluid, the drag function F_D can be written as follows [12]

$$F_D = \frac{1}{2}\rho_c A_d C_D |\mathbf{u}_{Cd}| \mathbf{u}_{Cd} \quad (2.34)$$

In the present work Virtual mass and Basset history terms are neglected. For calculating the relative velocity from the equation(2.32) we need to model the drag function f_{drag} from below relation.

$$f_d = \frac{C_D Re_d}{24} \quad (2.35)$$

There are different drag coefficient models depending on various factors. At small particle Reynolds number, the total drag coefficient is given by Stokes law [12]

$$C_{D,st} = \frac{24}{Re_d} \quad (2.36)$$

The particle Reynolds number Re_p is defined as follows

$$Re_d = \frac{d_d \rho_c |\mathbf{u}_{Cd}|}{\mu_c} \quad (2.37)$$

An often used expression for the drag coefficient is due to Schiller & Nauman [12]

$$\begin{aligned}
C_D &= \frac{24}{Re_d} (1 + 0.15 Re_d^{0.687}) & Re_d < 1000 \\
&= 0.44 & Re_d > 1000
\end{aligned} \tag{2.38}$$

Above equation is derived by considering single particle in a fluid. In a suspension, the influence of the distortion of the flow field is caused by the presence of other particles has to be taken into account. With in increase in particle concentration, a particle feels an increase in flow resistance which in turn leads to a higher drag coefficient. Alternate way, [11] the viscosity of the continuous phase in expressions for drag coefficient should be replaced by the apparent viscosity of the mixture μ_m . Their formulation for drag coefficient of solid particle is

$$\begin{aligned}
C_D &= \frac{24}{Re_d} (1 + 0.15 Re_d^{0.75}) & Re_d < 1000 \\
&= 0.45 \left\{ \frac{1 + 17.67 [f(\phi_d)]^{6/7}}{18.67 f(\phi_d)} \right\} & Re_d > 1000 \\
f(\phi_d) &= \sqrt{1 - \phi_d} \left(\frac{\mu_c}{\mu_m} \right) \\
Re_d &= \frac{d_d |\mathbf{u}_{Cd}| \rho_c}{\mu_m}
\end{aligned} \tag{2.39}$$

Ding & Gidaspow [14] equations for C_D for dense suspensions:

$$\begin{aligned}
C_D &= \frac{24}{\phi_c Re_d} (1 + 0.15 (\phi_c Re_d)^{0.687}) & \phi_c Re_d < 1000 \\
&= 0.44 & \phi_c Re_d > 1000
\end{aligned} \tag{2.40}$$

Each drag function has different β formulation (2.29).

2.2 Constitutive Equations

In order to have the field equations(2.7)(2.13)(2.19)(2.32)for the mixture model in a form suitable for applications, they have to be closed, i.e., constitutive models for various terms are required. This closure problem is often very difficult. Some of the closure equations are obvious consequences from the approach used in developing the field equations, Such as the definition of velocity and density of mixture.

Constitutive equations of the mixture models are not theoretically studied as extensively as those for full multiphase models.The approach of writing he closure laws directly in terms

of the mixture model parameters is more straightforward and consistent with derivation of the field equations[1].

saturation condition

When a mixture is fully saturated

$$\sum_{k=1}^n \phi_k = 1 \quad (2.41)$$

This was already used in deriving relation between various velocities indicates that computation of the volume fraction from the phase continuity equation can be omitted for one phase.

Mixture properties

The mixture density and viscosity is defined in (2.8)(2.9)

$$\rho_m = \sum_{k=1}^n \phi_k \rho_k \quad (2.42)$$

$$\mu_m = \sum_{k=1}^n \phi_k \mu_k \quad (2.43)$$

It has been discussed in the beginning.

Kinematic closure relations

By employing the diffusion and relative velocity relations the diffusion stresses can be expressed as the function of \mathbf{u}_{Cp} as follows

$$\tau_{Dm} = -\rho_m \sum_{k=1}^n C_k \mathbf{u}_{Ck} \mathbf{u}_{Ck} + \rho_m \sum_{k,l=1}^n C_k C_l \mathbf{u}_{Ck} \mathbf{u}_{Cl} \quad (2.44)$$

As we are doing for only one dispersed phase

$$\tau_{Dm} = -\rho_m C_d (1 - C_d) \mathbf{u}_{Cd} \mathbf{u}_{Cd} \quad (2.45)$$

Pressure differences

The properties of interface determine the pressure difference. With out any surface tension pressures of all the phases are taken to be equal .This assumption is customarily made

except in the case of expanding bubbles [10]. While deriving mixture momentum equation we assumed in (2.13) for pressure of the mixture that

$$\nabla p_m = \sum_{k=1}^n \phi_k \nabla p_k \quad (2.46)$$

Interfacial momentum conservation

The term M_m in the mixture momentum equation (2.13) denotes the mixture momentum source due to the surface tension and depends upon the geometry of the interface. In case of two phase flow, the mixture momentum source is given by [1]

$$M_m = \kappa_{kl} \sigma \nabla \phi_d + M_{Hm} \quad (2.47)$$

The first term of the right hand side is zero if the surface tension is neglected. The last term M_{Hm} represents the effect of changes in the mean curvature (reference), assumed that $M_{Hm} = 0$. Commonly and especially in practical applications, the mixture momentum source M_m is ignored [8][7].

Interfacial mass conservation

The balance equation for interfacial mass conservation is given by (2.6)

$$\sum_{k=1}^n \Gamma_k = 0 \quad (2.48)$$

If the phase changes does not occur the interfaces between the phases, $\Gamma_k = 0$

Viscous shear stress

The general form for the viscous shear stress tensor in Newtonian viscous fluid is

$$\boldsymbol{\tau} = \mu \left[\nabla \mathbf{u} + (\nabla \mathbf{u})^T \right] + \lambda (\nabla \cdot \mathbf{u}) \mathbf{I} \quad (2.49)$$

where λ is the second viscosity coefficient and \mathbf{I} is the unit tensor. The Stokes relation,

$$\lambda = -\frac{2}{3}\mu \quad (2.50)$$

is generally assumed to be valid. The term involving the shear stress tensor in the Navier Stokes equation would be

$$\nabla \cdot \boldsymbol{\tau} = \mu \left[\nabla^2 \mathbf{u} + \frac{1}{3} \nabla (\nabla \cdot \mathbf{u}) \right] \quad (2.51)$$

where a constant viscosity coefficient μ is assumed. For a single incompressible fluid

$$\nabla \cdot \mathbf{u} = 0 \quad (2.52)$$

Accordingly last terms of (2.51) can be ignored. In multiphase flow (2.52) it is not necessary valid for an individual phase. The divergence of mixture velocity is neither generally equal to zero.

The total viscous stress for a multiphase mixture can be represented as a sum of the contribution of the individual phases (2.51) present in the mixture.

$$\boldsymbol{\tau}_m = \sum_{k=1}^n \phi_k \mu_k \left\{ [\nabla \mathbf{u}_k + (\nabla \mathbf{u}_k)^T] \right\} \quad (2.53)$$

Representing phase velocity in terms of the mixture and diffusion velocities, the viscous shear stress tensor for the mixture can be written as follows:

$$\boldsymbol{\tau}_m = \sum_{k=1}^n \phi_k \mu_k \left\{ [\nabla \mathbf{u}_k + (\nabla \mathbf{u}_k)^T] \right\} + \sum_{k=1}^n \phi_k \mu_k \left\{ [\nabla \mathbf{u}_{Mk} + (\nabla \mathbf{u}_{Mk})^T] \right\} \quad (2.54)$$

Compare to the formulation for single phase flow, the viscous stress in a mixture has a additional term caused by relative motion. This term is often small and, when drift velocity is constant, it can even ignored. The viscosity of the mixture is

$$\mu_m = \sum_{k=1}^n \phi_k \mu_k \quad (2.55)$$

Considering the contribution of one phase to the viscous stress term of the mixture momentum equation, we obtain

The closure law for viscous term of mixture can be determined analogously to single phase flow in terms of mixture parameters

$$\boldsymbol{\tau}_m = \mu_m \left[\nabla \mathbf{u}_m + (\nabla \cdot \mathbf{u}_k) - \frac{2}{3} (\nabla \cdot \mathbf{u}_m) I \right] \quad (2.56)$$

where μ_m is the dynamic viscosity for mixture. And is often assumed that $\nabla \cdot \mathbf{u}_m = 0$.

2.3 summary

In the following, a summary the mixture model equations is presented for case of one dispersed phase p for laminar flows.

$$\frac{\partial}{\partial t}\rho_m + \nabla \cdot (\rho_m \mathbf{u}_m) = 0 \quad (2.57)$$

$$\begin{aligned} \frac{\partial}{\partial t}(\rho_m \mathbf{u}_m) + \nabla \cdot (\rho_m \mathbf{u}_m \mathbf{u}_m) = & -\nabla p_m + \rho_m g + \mu_m [\nabla \mathbf{u}_m + (\nabla \mathbf{u}_m)^T] \\ & -\nabla \cdot [\rho_m C_d (1 - C_d) \mathbf{u}_{Cd} \mathbf{u}_{Cd}] \end{aligned} \quad (2.58)$$

$$\frac{\partial \phi_d}{\partial t} + \nabla \cdot (\phi_d \mathbf{u}_m) = -\nabla \cdot [\phi_d (1 - C_d) \mathbf{u}_{Cd}] \quad (2.59)$$

In above equations(2.58)(2.59) the phase slip terms are expressed explicitly as function of the relative velocity, rather than diffusion velocity. The relative velocity is obtained from the generalized equation

$$\mathbf{u}_{Cd} = \frac{\tau_d}{f_{drag}} \frac{(\rho_d - \rho_m)}{\rho_p} \left[g - (\mathbf{u}_m \cdot \nabla) \mathbf{u}_m - \frac{\partial \mathbf{u}_m}{\partial t} \right] \quad (2.60)$$

where the particles are assumed to be spherical and the fluctuation in slip velocities are ignored as the principle contributors of turbulence are turbulent stress term in momentum equation. For laminar flow set of equations is now complete. Empirical correlations have to be used for the quantities C_D and μ_m . If multiple dispersed phases are present, the mixture model equations are not simple. The continuity equation is solved for each dispersed phase. Determining the relative velocity becomes more complicated because the hindrance effects of the particles of the other phases need to be taken into account[29]. Mixture including several particle phases with different material densities can be considered as above. The formulation applies also if the density of the material of the dispersed phase is constant but the particle size varies. Particles are classified according to their size and each group is considered as a separate phase.

Chapter 3

Discretization of Equations

Solver named as **Thunderstorm** is based on the Anupravah 2 developed by Dr. Amaresh Dalal and Prof. Vinayak Eswaran. The development of 3D unstructured code with single phase is carried out by Vatsalya Sharma[2] and Dr. Raja Banerjee. It is a semi implicit solver capable of handling unstructured grids. Its ability to read grid in CGNS format and write the results in same. It has a text based interface (TBI) and most of the files are written in C language.

3.1 Solution algorithm

The final discretized form of the governing differential equations are:

Continuity: The continuity equation is discretized as follows,

$$\sum_f F_f^{n+1} = 0 \quad (3.1)$$

where

$$F_f = u_f^{n+1} S_{fx} + v_f^{n+1} S_{fy} + w_f^{n+1} S_{fz} \quad (3.2)$$

S_{fx} denotes area of f face and x component of it. **Momentum:** The momentum Equation is discretized as follows

$$\begin{aligned} V_p \frac{(\rho_{m,p} u_p)^{n+1} - (\rho_{m,p} u_p)^n}{\Delta t} + \sum_f F_f^{n+1} u_f^{n+1} + \sum_f F_{duf}^{n+1} = \\ - \sum_f p_f^{n+1} S_{fx} + (S_u)_p V_p \end{aligned} \quad (3.3)$$

$$V_p \frac{(\rho_{m,p} v_p)^{n+1} - (\rho_{m,p} v_p)^n}{\Delta t} + \sum_f F_f^{n+1} v_f^{n+1} + \sum_f F_{df}^{n+1} = - \sum_f p_f^{n+1} S_{fy} + (S_v)_p V_p \quad (3.4)$$

$$V_p \frac{(\rho_{m,p} w_p)^{n+1} - (\rho_{m,p} w_p)^n}{\Delta t} + \sum_f F_f^{n+1} w_f^{n+1} + \sum_f F_{df}^{n+1} = - \sum_f p_f^{n+1} S_{fz} + (S_w)_p V_p \quad (3.5)$$

Volume Fraction: The Volume Fraction Equation is discretized as follows

$$V_p \frac{(\rho_{k,p} \phi_p)^{n+1} - (\rho_{k,p} \phi_p)^n}{\Delta t} + \sum_f F_{k,f}^{n+1} \phi_f^{n+1} \sum_f F_{df}^{n+1} = (S_u)_p V_p \quad (3.6)$$

where subscript p denotes the value of variable at the cell center in current cell. As we are taking diffusion equal to zero last term in LHS is omitted. where $(n + 1)$ denotes the unknown value of the current time step

In the present study, the Navier stokes and volume fraction equations are solved using the finite volume method. We have used collocated grid arrangement, where the dependent variables are calculated from the centroid of the finite volume. This arrangement produces pressure velocity decoupling(refer patankar and vatsalya thesis). The solution to this problem is explained in the thesis of Vatsalya Sharma [2].

3.1.1 SemiImplicit Algorithm

In semi Implicit algorithm the Navier stokes and Volume Fraction equations are solved using flux and mixture density value of the previous step. This eliminates the need for flux convergence loop, decreasing the amount of time taken to achieve convergence. As both Implicit and Semi Implicit algorithm are first order accurate in time, semi Implicit algorithm gives acceptable results even for unsteady problems. Initial condition for velocity and pressure are prescribed at all points in the domain and boundary conditions are defined at the start of the problem.

Step 0: Initialize all the variables to their respective initial conditions.

Step 1: Evaluate the Mass velocities, u_* , by solving the "Mass velocity equation" which is basically the Navier Stokes equation but without the pressure term. These are given by,

$$V_p \frac{(\rho_{m,p} u_p)^* - (\rho_{m,p} u_p)^n}{\Delta t} + \sum_f F_f^n u_f^* + \sum_f F_{df}^* = (S_u)_p V_p \quad (3.7)$$

$$V_p \frac{(\rho_{m,p} v_p)^* - (\rho_{m,p} v_p)^n}{\Delta t} + \sum_f F_f^n v_f^* + \sum_f F_{dvf}^* = (S_v)_p V_p \quad (3.8)$$

$$V_p \frac{(\rho_{m,p} w_p)^* - (\rho_{m,p} w_p)^n}{\Delta t} + \sum_f F_f^n w_f^* + \sum_f F_{dwf}^* = (S_w)_p V_p \quad (3.9)$$

Usually the source terms are lagged to the values of the previous time step. And the flux of the previous time step are being used here.

Step 2: Calculate the mass flux at the each face of the control volume using the newly evaluated mass velocity values.

$$F_f^* = \rho_f \cdot u_f^* \cdot S_f \quad (3.10)$$

$$u_f^* = \frac{V_p u_n^* + V_n u_p^*}{V_p + V_n} \quad (3.11)$$

$$\rho_f^* = \frac{V_p \rho_n^* + V_n \rho_p^*}{V_p + V_n} \quad (3.12)$$

Step 3: Evaluate the values of pressure at $(n + 1)^{th}$ time step using the pressure poisson equation,

$$\sum_f (\nabla p_f^{n+1}) \cdot S_f = \frac{1}{\Delta t} \sum_f F_f^* \quad (3.13)$$

Step 4: Calculate the mass flux of $(n + 1)^{th}$ time step using the expression

$$F_f^{n+1} = F_f^* - \Delta t (\nabla p_f^{n+1}) \cdot S_f \quad (3.14)$$

Now that the mass flux will satisfy continuity.

Step 5: Now we solve the complete Navier Stokes equation given by,

$$V_p \frac{(\rho_{m,p} u_p)^{n+1} - (\rho_{m,p} u_p)^n}{\Delta t} + \sum_f F_f^n u_f^{n+1} + \sum_f F_{duf}^{n+1} = - \sum_f p_f^{n+1} S_{fx} + (S_u)_p V_p \quad (3.15)$$

$$V_p \frac{(\rho_{m,p} v_p)^{n+1} - (\rho_{m,p} v_p)^n}{\Delta t} + \sum_f F_f^n v_f^{n+1} + \sum_f F_{dvf}^{n+1} = - \sum_f p_f^{n+1} S_{fy} + (S_v)_p V_p \quad (3.16)$$

$$V_p \frac{(\rho_{m,p} w_p)^{n+1} - (\rho_{m,p} w_p)^n}{\Delta t} + \sum_f F_f^n w_f^{n+1} + \sum_f F_{dwf}^{n+1} = - \sum_f p_f^{n+1} S_{fz} + (S_w)_p V_p \quad (3.17)$$

After convergence we the values of u^{n+1} , v^{n+1} , w^{n+1} , these are the current time step velocity values. Here all the fluxes are taken from the previous time step values. The source terms are usually lagged to the previous time step values.

Step 6: After this we solve for scalar in this case we solve volume fraction equation given by,

$$V_p \frac{(\rho_{k,p} \phi_p)^{n+1} - (\rho_{k,p} \phi_p)^n}{\Delta t} + \sum_f F_{k,f}^{n+1} \phi_f^{n+1} = (S_u)_p V_p \quad (3.18)$$

Step 7: After getting scalar values we use to update the density and dynamic viscosity values.

$$\rho_m = \sum_{k=1}^n \alpha_k \rho_k \quad (3.19)$$

$$\mu_m = \sum_{k=1}^n \alpha_k \mu_k \quad (3.20)$$

Step 8: Now we find the slip velocity which are added in the source term of momentum and volume fraction equations.

$$\mathbf{u}_{Cp} = \frac{\tau_p}{f_{drag}} \frac{(\rho_p - \rho_m)}{\rho_p} \left[g - (\mathbf{u}_m \cdot \nabla) \mathbf{u}_m - \frac{\partial \mathbf{u}_m}{\partial t} \right] \quad (3.21)$$

Step 8: If it is a steady state problem, check whether velocities and scalars are converged to required level of accuracy. If not converged then set $u^{n+1} \rightarrow u^n$, $F^{n+1} \rightarrow F^n$, $\phi^{n+1} \rightarrow \phi^n$, $t \rightarrow t + \Delta t$ and go to step 1. If it is unsteady problem the continue as many time steps as needed.

Source Terms

We have added, relative velocity flux terms in mixture momentum equation (2.58) and volume fraction equation of disperse phase (2.59) to source terms for corresponding equations. The relative velocity terms are computed from previous time step values. The respective source terms are:

$$\mathbf{S}_{momentum} = - \sum_f F_{Rel,f} \mathbf{u}_{cd,f} \quad (3.22)$$

$$\mathbf{S}_{volfrac} = - \sum_f F_{vol,f} \phi_d \quad (3.23)$$

where the subscript d is used to denote the dispersed phase , $\mathbf{S}_{momentum}$ is the source term and $F_{Rel,f}$ is the relative velocity flux of mixture momentum equation. $\mathbf{S}_{volfrac}$ is source term and $F_{vol,f}$ is the relative velocity flux in volume fraction equation of dispersed phase. The ϕ_d is the volume fraction of the dispersed phase. Both the flux terms have different formulations, the flux term in mixture momentum equation is given by

$$F_{Rel,f} = \rho_{m,f} C_{df} (1 - C_{df}) [u_{cd,f} \cdot S_{fx} + v_{cd,f} \cdot S_{fy} + w_{cd,f} \cdot S_{fz}] \quad (3.24)$$

The flux term in volume fraction equation is

$$F_{vol,f} = (1 - C_{df}) [u_{cd,f} \cdot S_{fx} + v_{cd,f} \cdot S_{fy} + w_{cdf} \cdot S_{fz}] \quad (3.25)$$

where the C_d is from the equation (2.22). The calculation of above variable at the face centers have been mentioned in the Appendix.

3.2 Closure

The discretization of the equations according to unstructured grid are mention in thesis of Vatsalya Sharma [2]. And the discretization of relative velocity terms in momentum and volume fraction equations are mentioned in Appendix.

Chapter 4

Laminar Validation of Multiphase Module

4.1 Introduction

The code results are compared with the Fluent for Laminar flows. In all the cases, we used Jet problems to validate. The validation is done for different density ratios (secondary phase to primary phase) and different Reynolds number with varying loading. In all the simulations, viscosity ratio (secondary phase to primary phase) is kept constant and particle size is taken to be $70\mu m$.

The domain size of our problem is $1 \times 1 \times 5$ with 1.2 million cells. Results are compared on YZ plane shown in figure (figure number) and values of X,Y,Z components of velocity taken from the central line of the plane. They are compared to Fluent results at different time levels. In this problem, a mixture of fluids is injected from inlet in to a tube with boundary conditions mentioned below.

Boundary Conditions

Inlet: The Mixture is injected in the Z direction, so the Dirichlet boundary condition to Z component of velocity and homogeneous Dirichlet boundary condition to remaining components $u = v = 0, w = constant$. Pressure has uniform Neumann boundary condition $\frac{\partial p}{\partial n} = 0$. Volume fraction has Dirichlet boundary condition $\phi = constant$.

Sides: The homogeneous Dirichlet boundary condition to all components of velocity $u = v = w = 0$. Pressure and volume fraction have uniform Neumann boundary condition $\frac{\partial p}{\partial n} = 0, \frac{\partial \phi}{\partial n} = 0$.

Outlet: Volume fraction and all the components of velocity have uniform Neumann boundary condition $\frac{\partial u}{\partial n} = 0, \frac{\partial v}{\partial n} = 0, \frac{\partial w}{\partial n} = 0, \frac{\partial \phi}{\partial n} = 0$. Pressure has homogeneous Dirichlet boundary condition $p = 0$.

Simulations are done on following domain

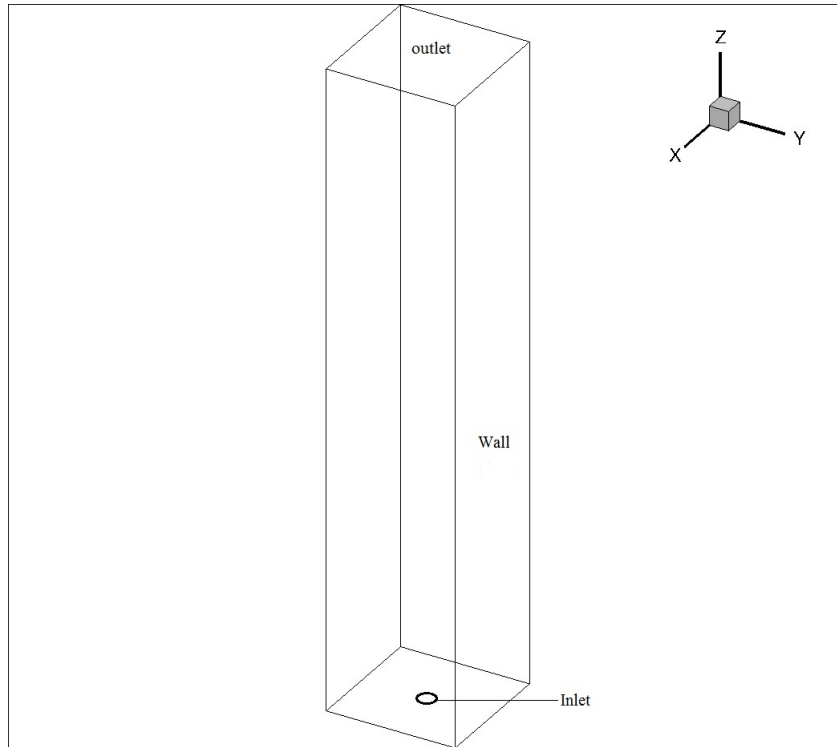


Figure 4.1: Domain

4.2 Different Density Ratios

Code is validated with different density ratios 1.1, 10, 100 with Reynolds number(Re) ranging from 100, 500, 1000, different volume fraction(VF) 0.1, 0.2, 0.3, 0.4 of secondary phase at the inlet.

4.2.1 Density ratio 1.1

Results for density ratio 1.1 is validated with the Fluent are mentioned below. As we are doing transient problem, values are compared at 1, 1.5, 2, 2.4 seconds.

The contour of Velocity Z and volume fraction are shown in figure 4.2,4.3 for $Re = 100$. Comparison is done for X, Y, Z velocities of mixture and Volume fraction of secondary phase.

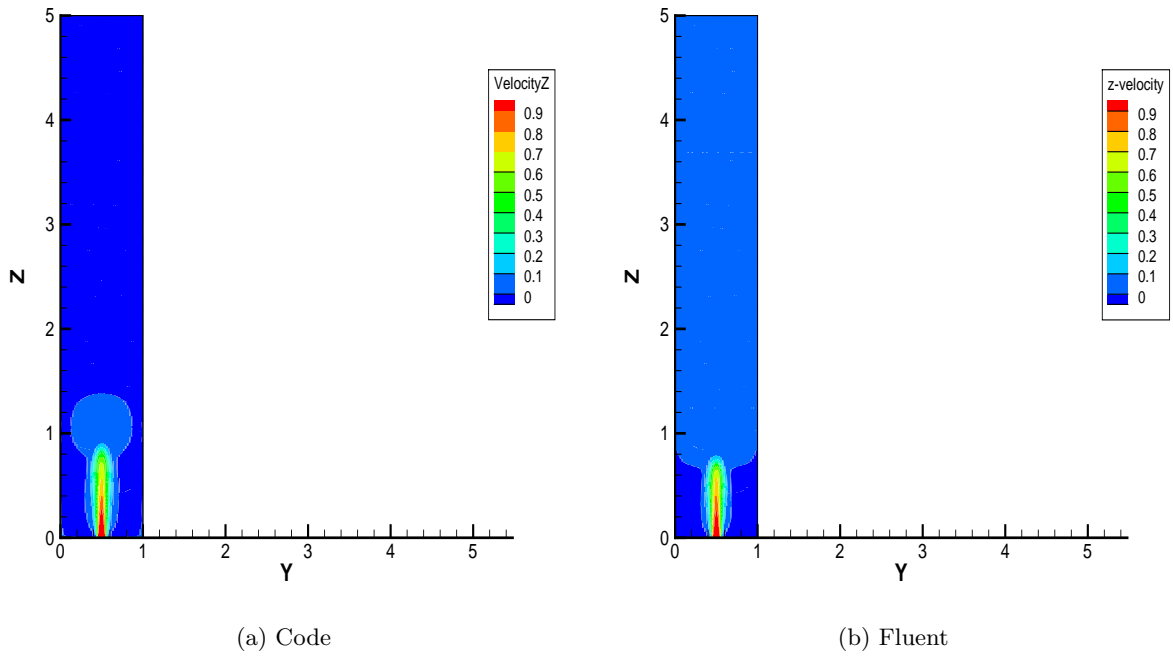


Figure 4.2: Contour of Velocity Z of mixture on YZ plane

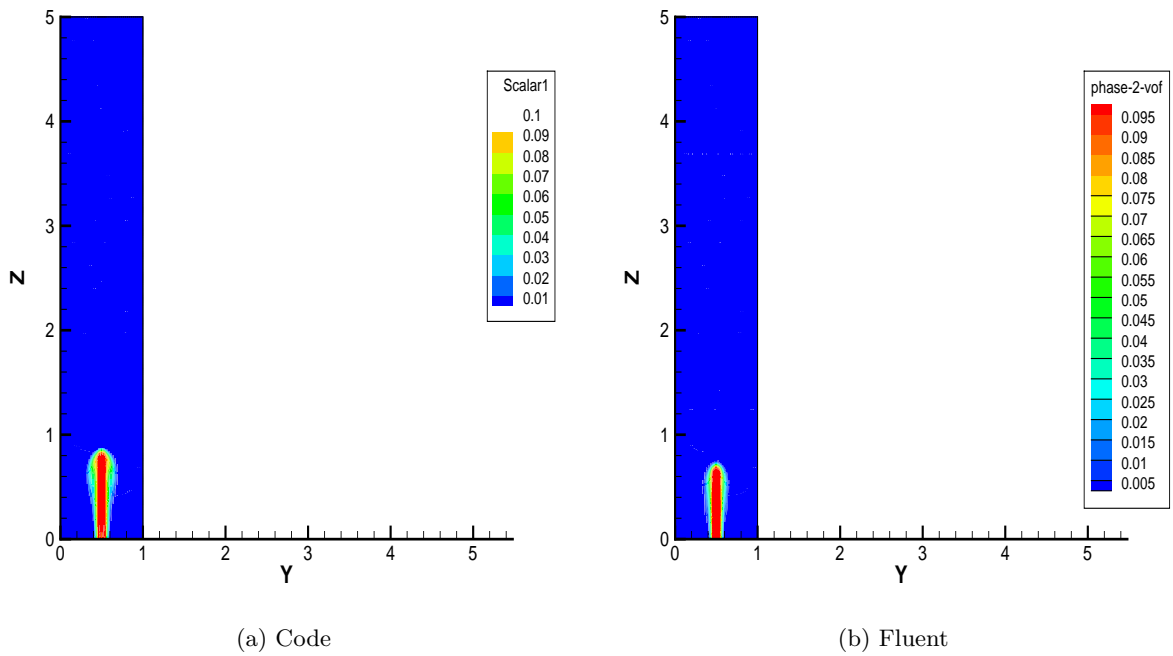


Figure 4.3: Contour of Volume fraction(VF) of secondary phase on YZ plane

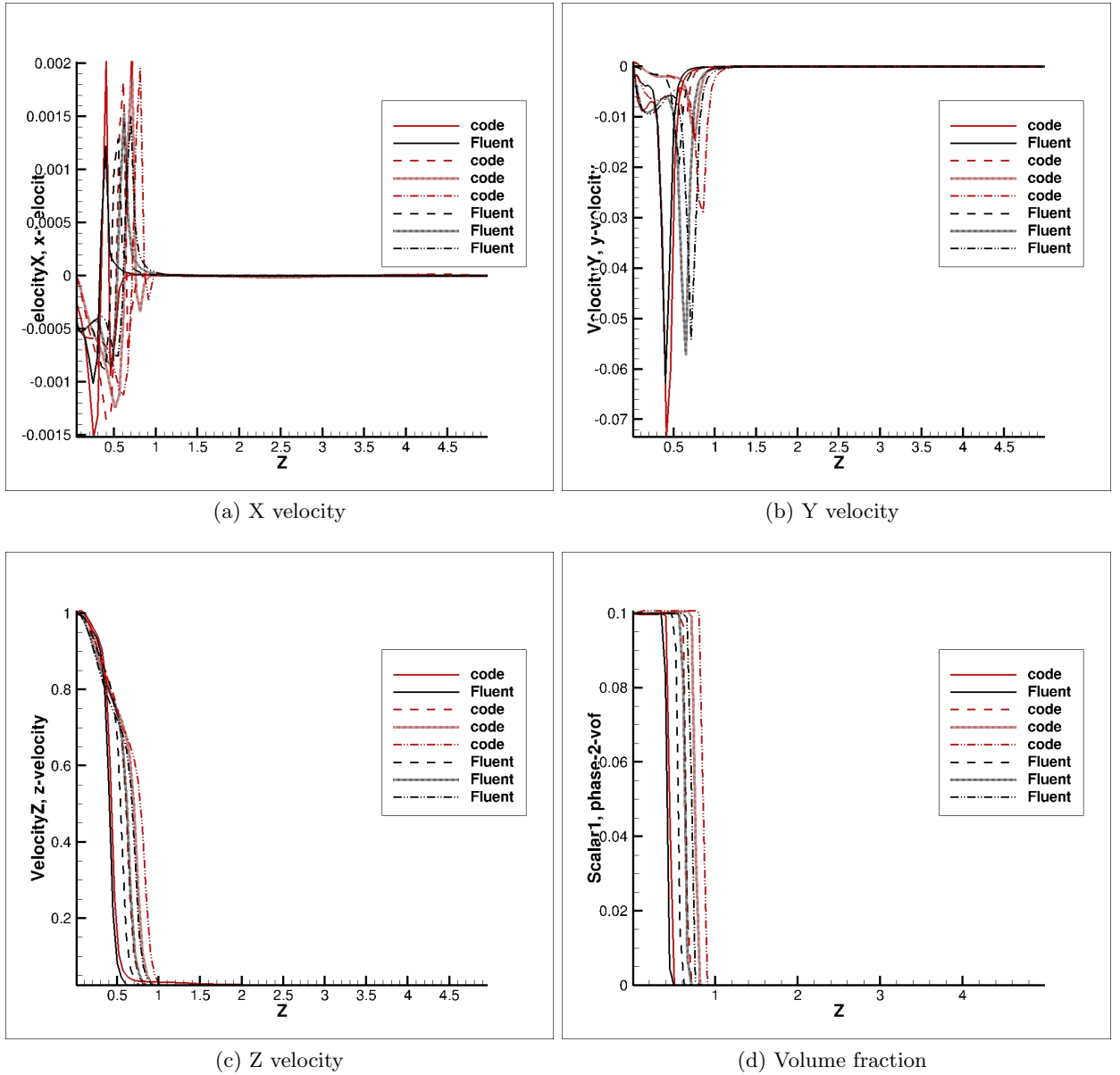
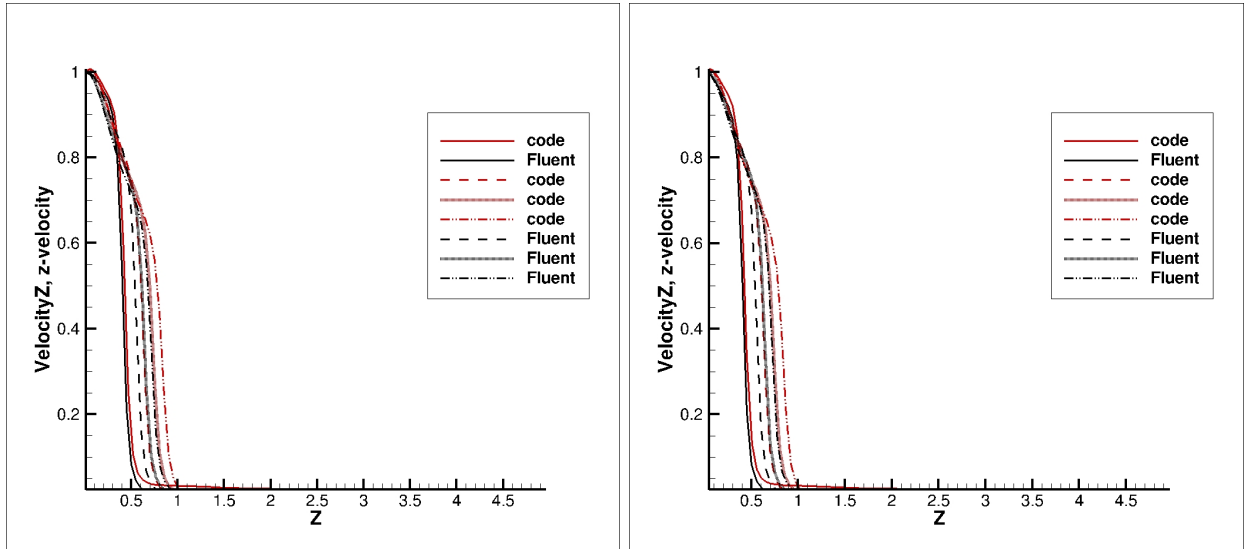


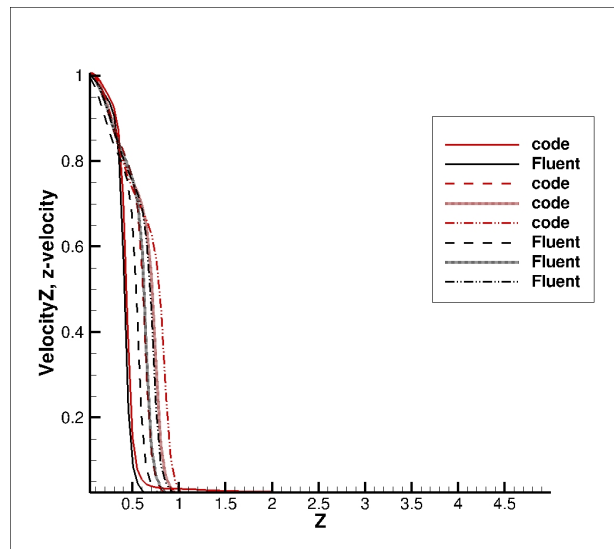
Figure 4.4: Comparison of code to Fluent for $Re = 100$ and $VF = 0.1$ for density ratio 1.1,

As velocity Z is more dominating figure 4.4 , further comparisons are done for only velocity Z. The difference in value of the code and Fluent is increasing as time progress. Further simulations are done for $Re = 100$ for different volumetric loading (VF). For all figures similar line pattern represents same time.



(a) $VF=0.1$

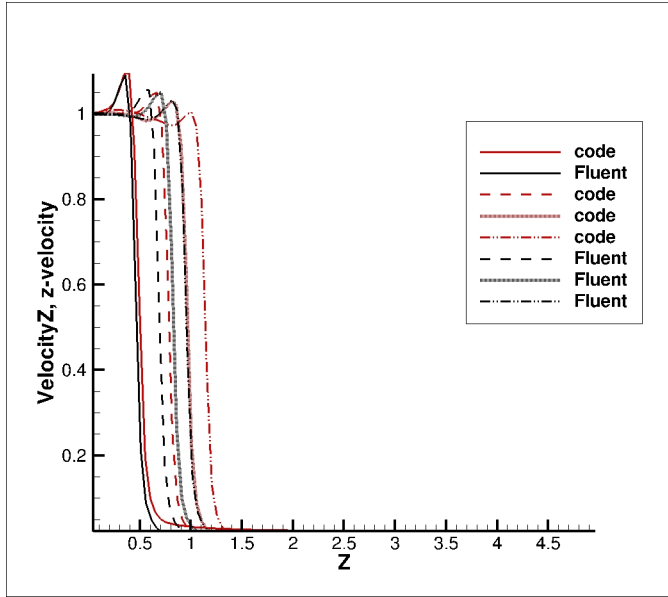
(b) $VF=0.2$



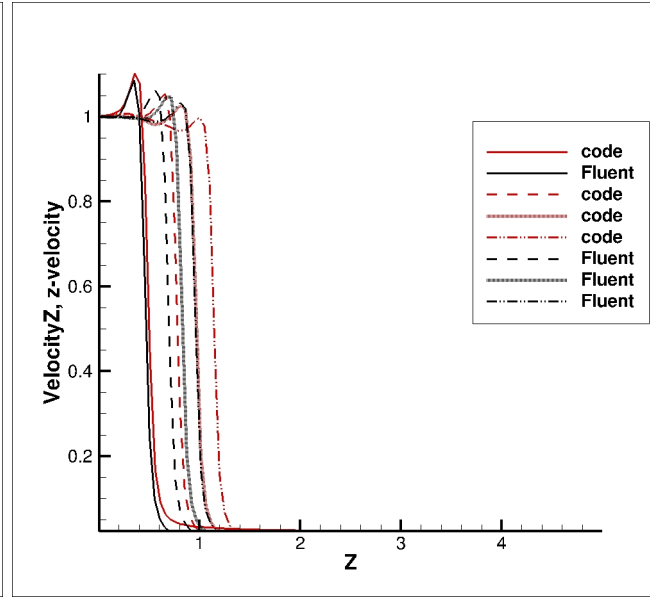
(c) $VF=0.3$

Figure 4.5: Comparison of Velocity Z for $Re = 100$ and $VF = 0.1, 0.2, 0.3, 0.4$ for density ratio 1.1,

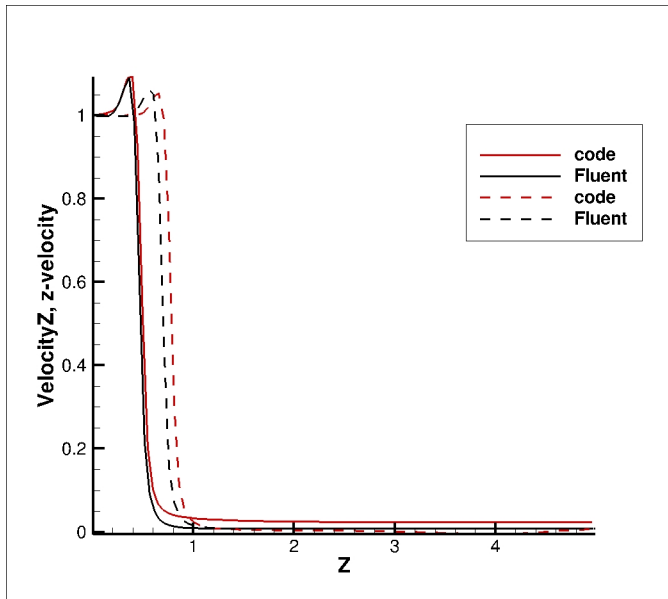
From figure 4.5 it can be noticed that difference in values increasing, as volumetric loading increases and also if time progresses. Similar pattern is observed in figure 4.6,4.7.



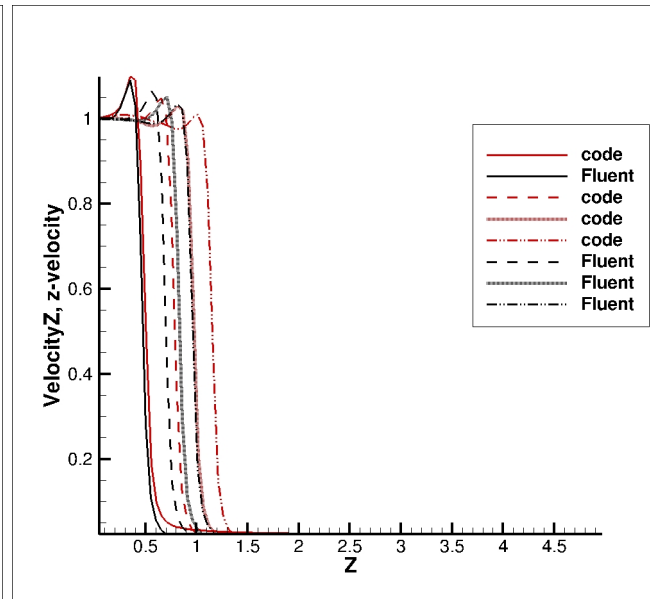
(a) $VF=0.1$



(b) $VF=0.2$

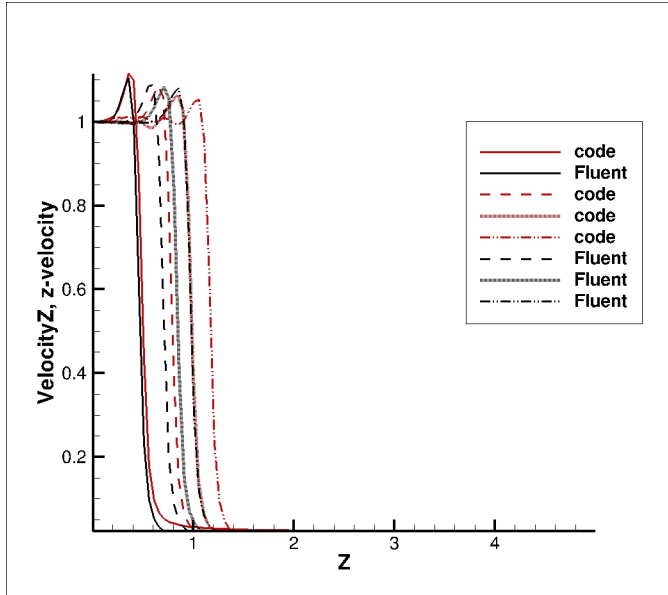


(c) $VF=0.3$

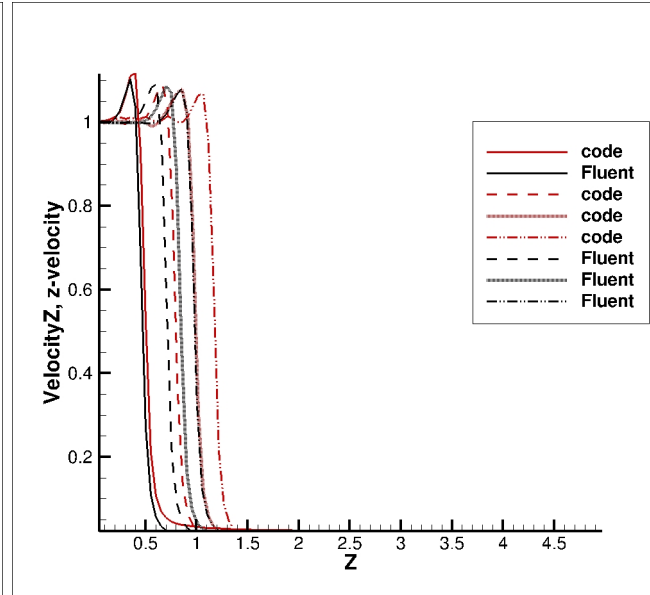


(d) $VF=0.4$

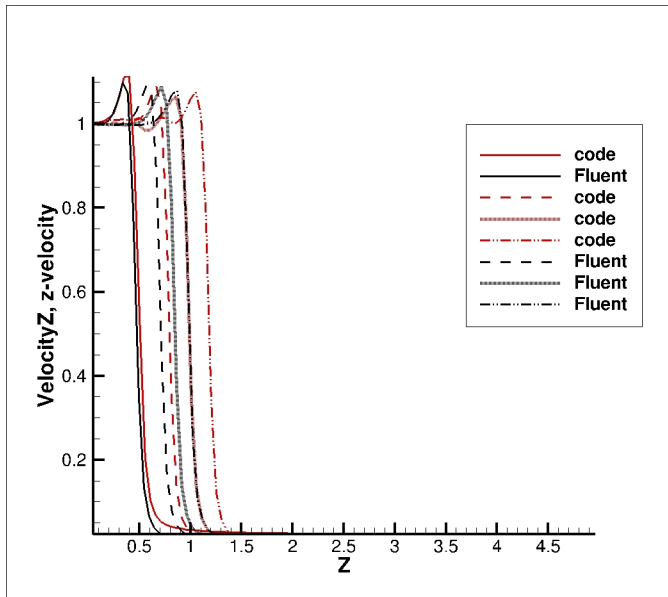
Figure 4.6: Comparison of Velocity Z for $Re = 500$ and $VF = 0.1, 0.2, 0.3, 0.4$ for density ratio 1.1,



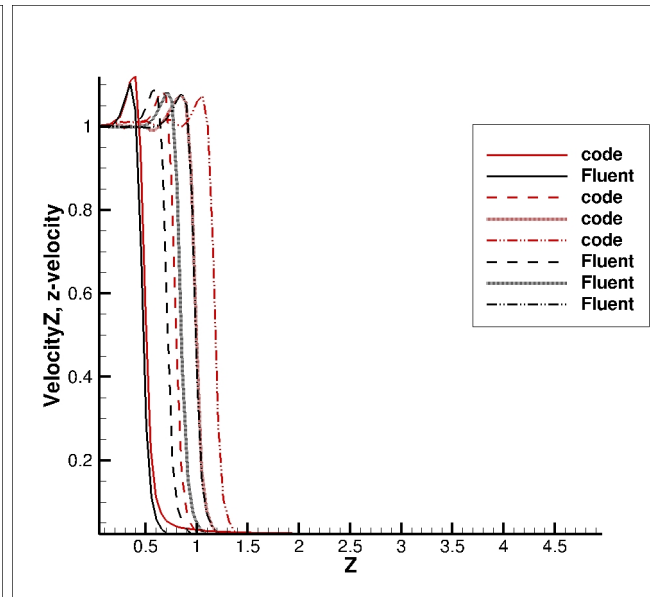
(a) $VF=0.1$



(b) $VF=0.2$



(c) $VF=0.3$



(d) $VF=0.4$

Figure 4.7: Comparison of Velocity Z for $Re = 1000$ and $VF = 0.1, 0.2, 0.3, 0.4$ for density ratio 1.1,

4.2.2 Density ratio 10:

From the figure 4.8,4.9,4.10, observed that difference between the values of code and Fluent not only increase with time, volumetric loading but also with Reynolds number.

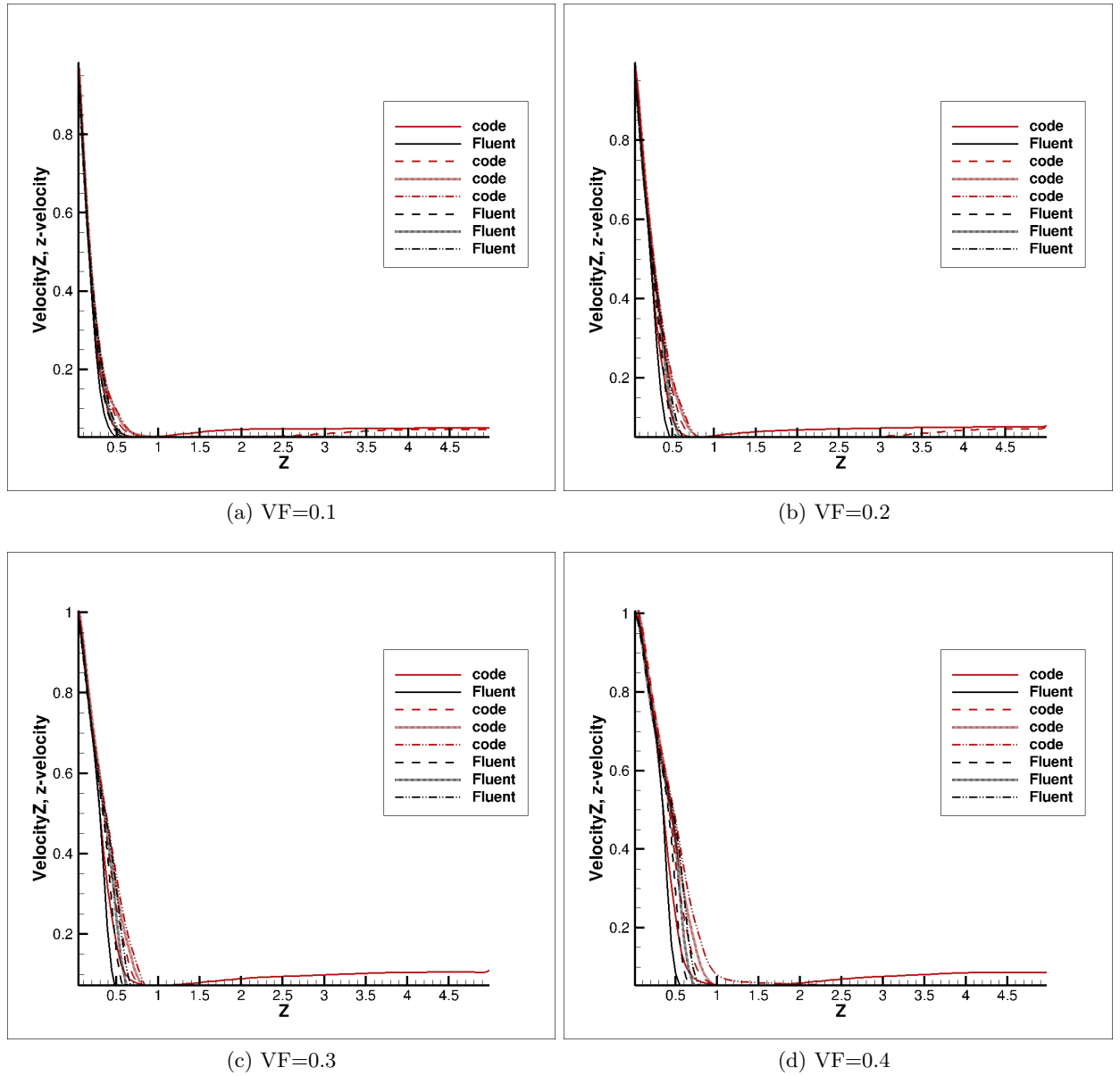
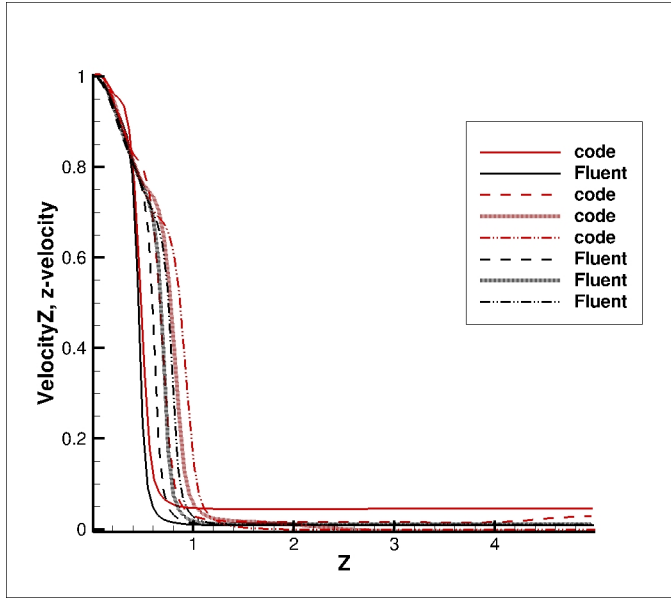
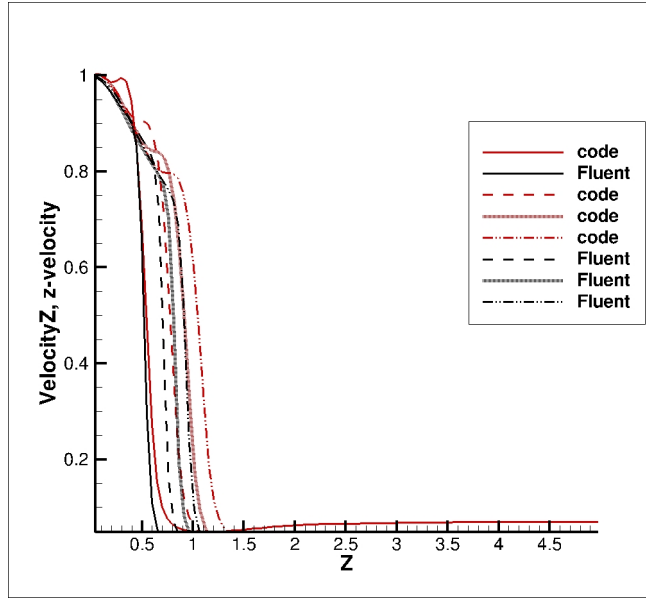


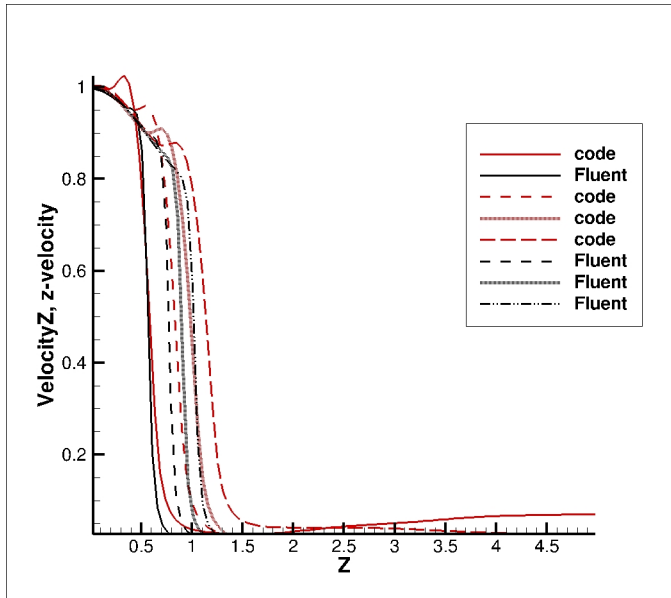
Figure 4.8: Comparison of Velocity Z for $Re = 100$ and $VF = 0.1, 0.2, 0.3, 0.4$ for density ratio 10



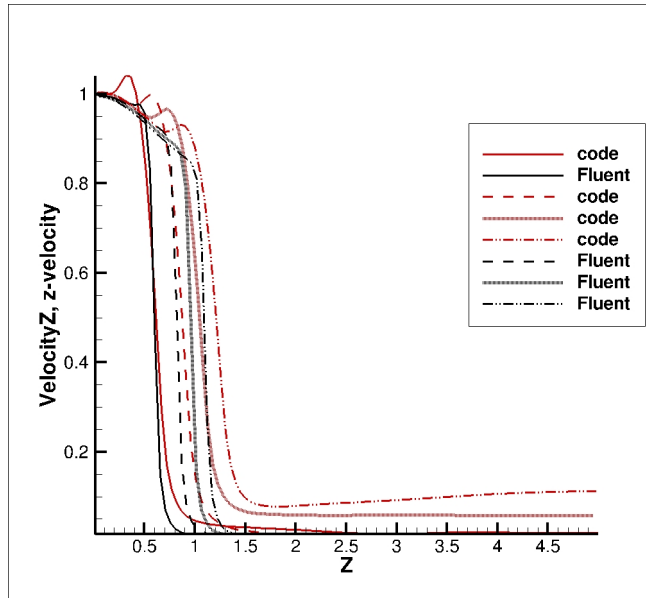
(a) $VF=0.1$



(b) $VF=0.2$

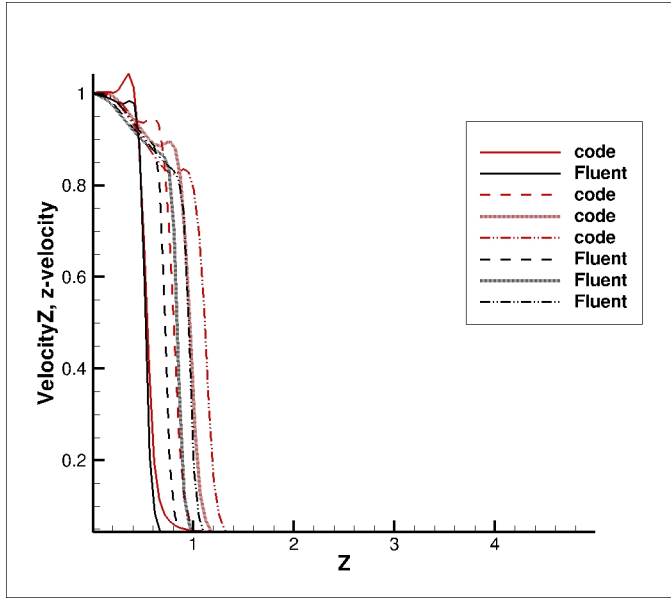


(c) $VF=0.3$

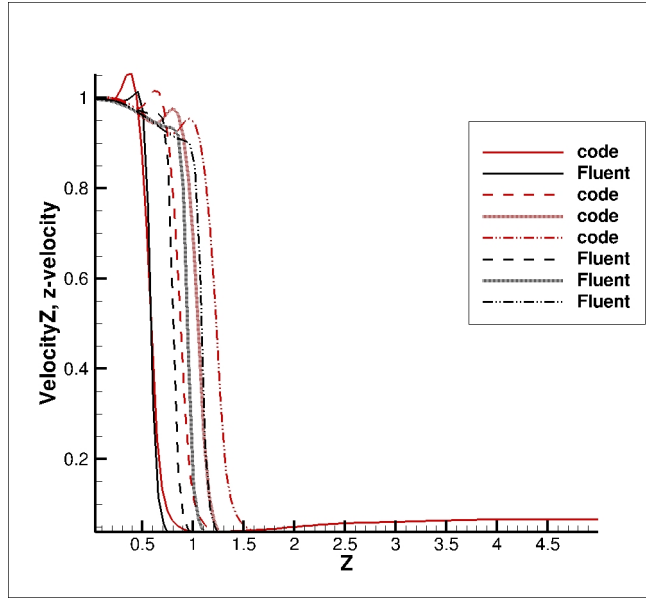


(d) $VF=0.4$

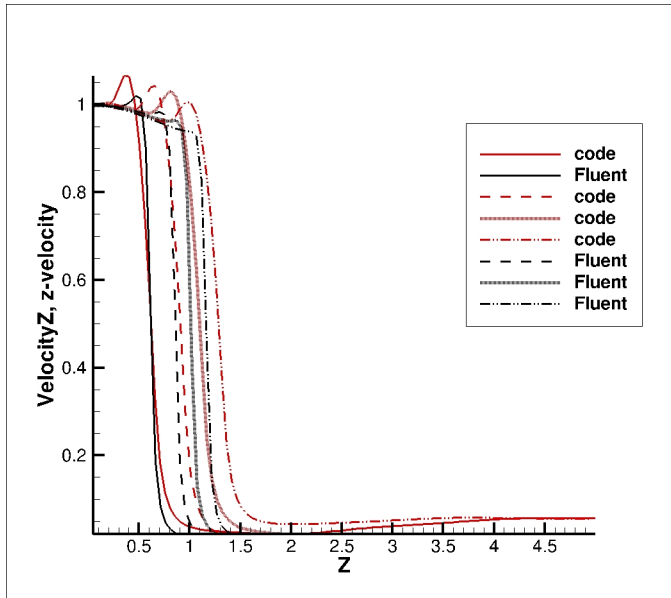
Figure 4.9: Comparison of Velocity Z for $Re = 500$ and $VF = 0.1, 0.2, 0.3, 0.4$ for density ratio 10



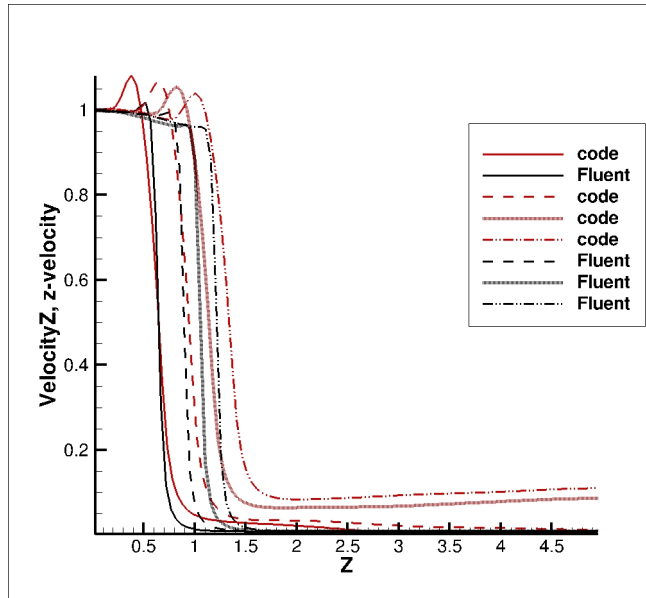
(a) $VF=0.1$



(b) $VF=0.2$



(c) $VF=0.3$



(d) $VF=0.4$

Figure 4.10: Comparison of Velocity Z for Re_{1000} and $VF = 0.1, 0.2, 0.3, 0.4$ for density ratio 10

4.2.3 Density ratio 100

From the figure 4.11,4.12,4.13, code is diverging from Fluent across the section.

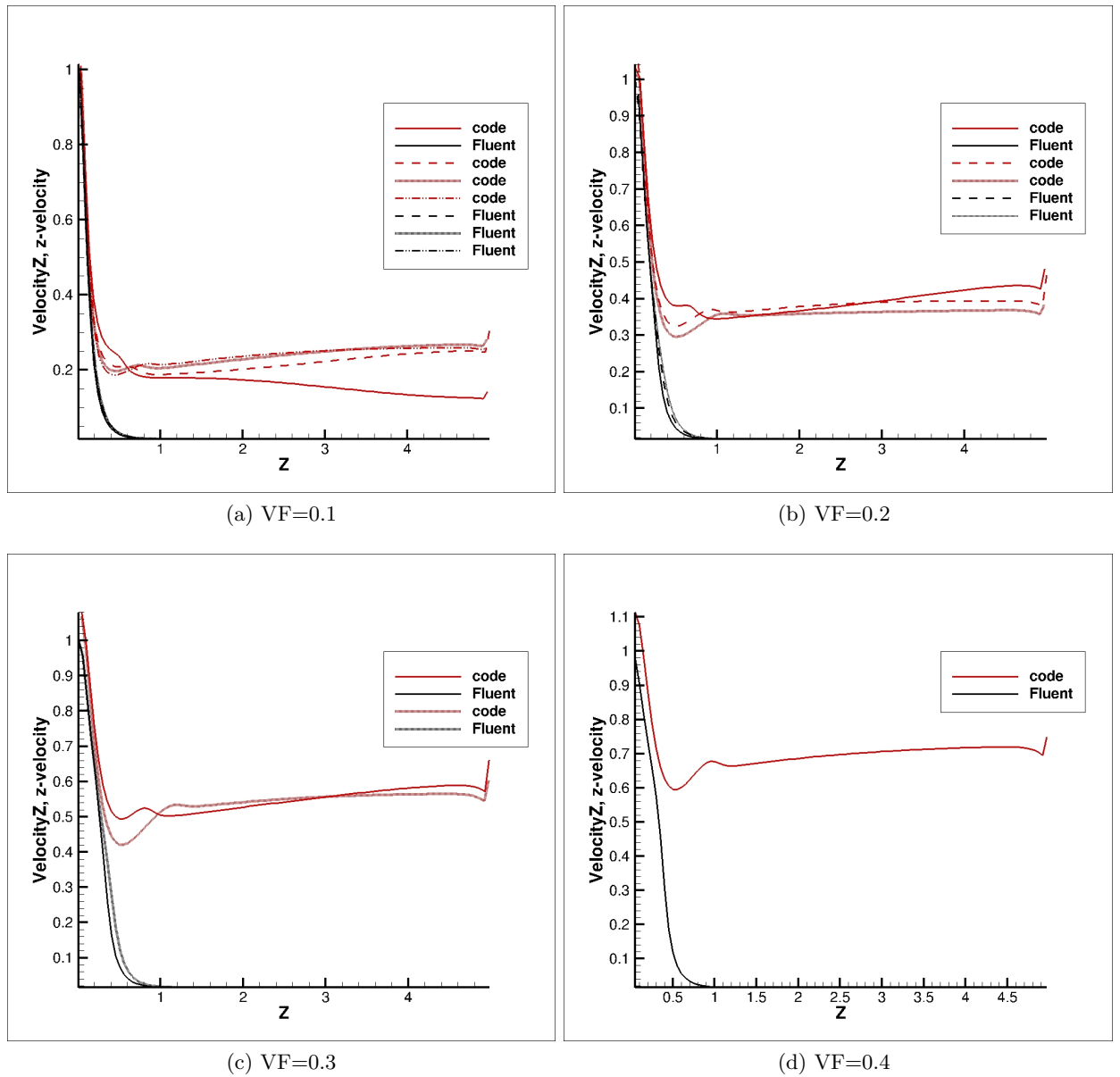
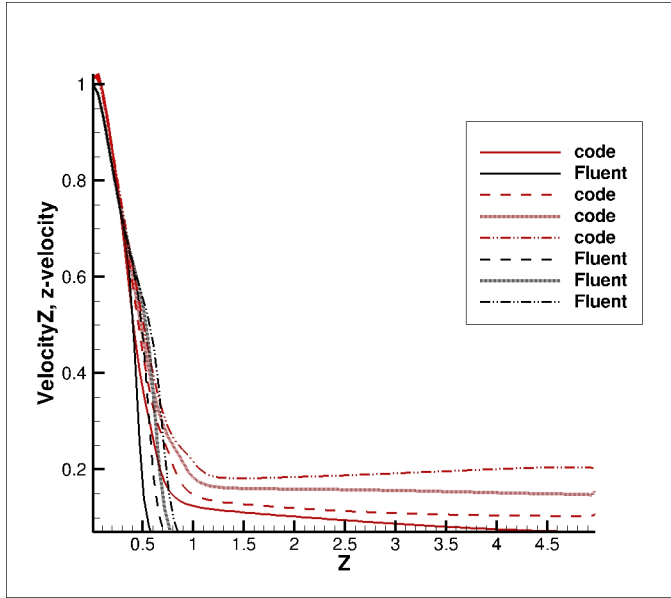
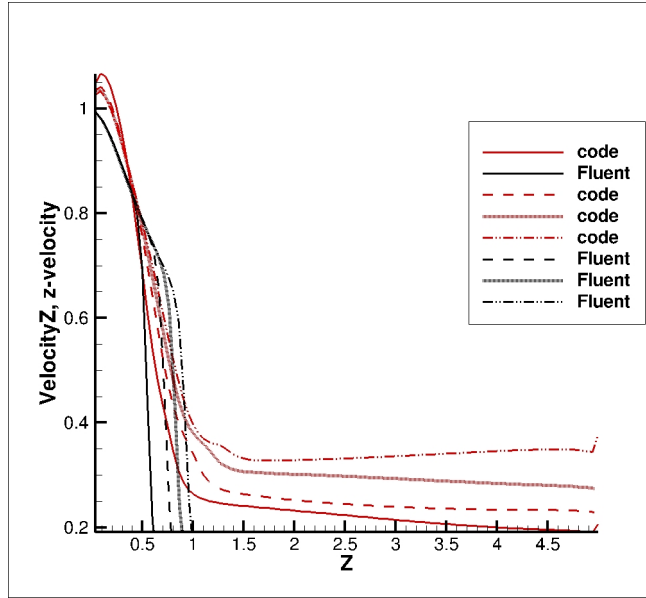


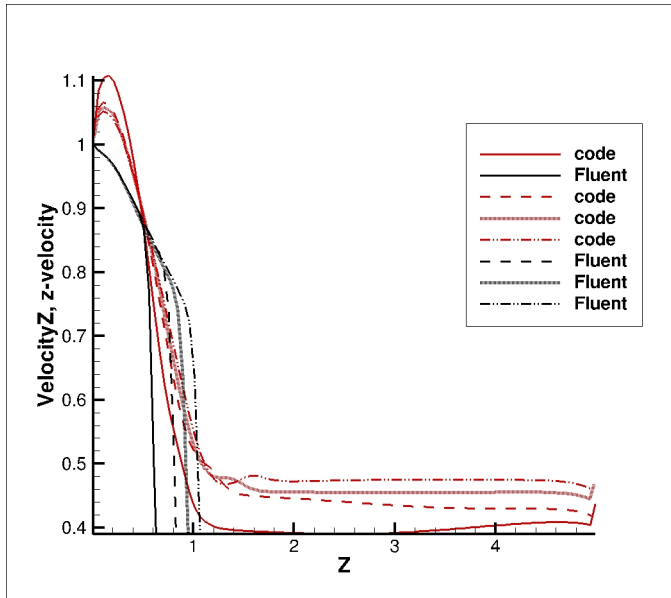
Figure 4.11: Comparison of Velocity Z for $Re = 100$ and $VF = 0.1, 0.2, 0.3, 0.4$ for density ratio 100,



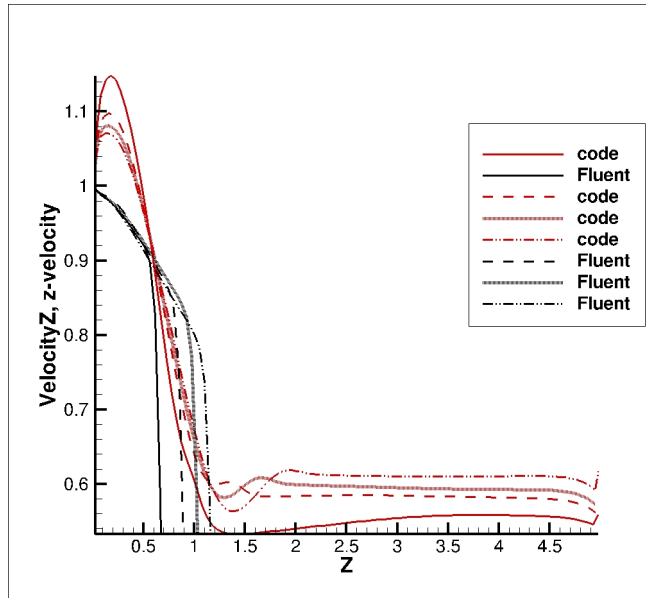
(a) $VF=0.1$



(b) $VF=0.2$

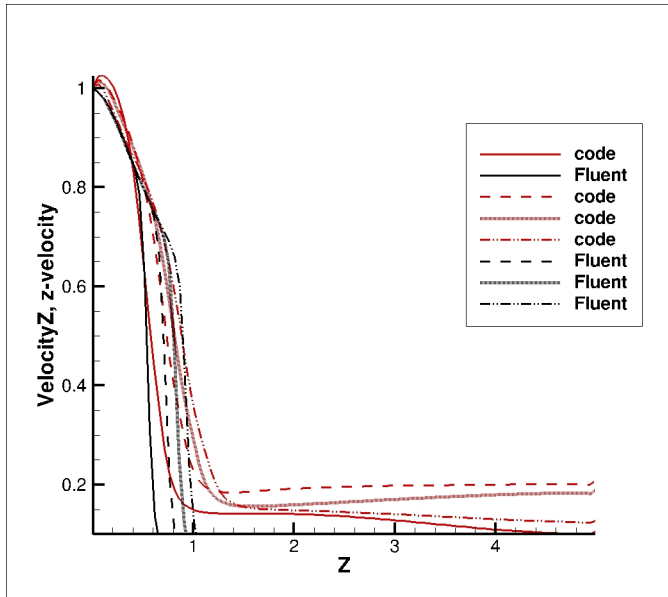


(c) $VF=0.3$

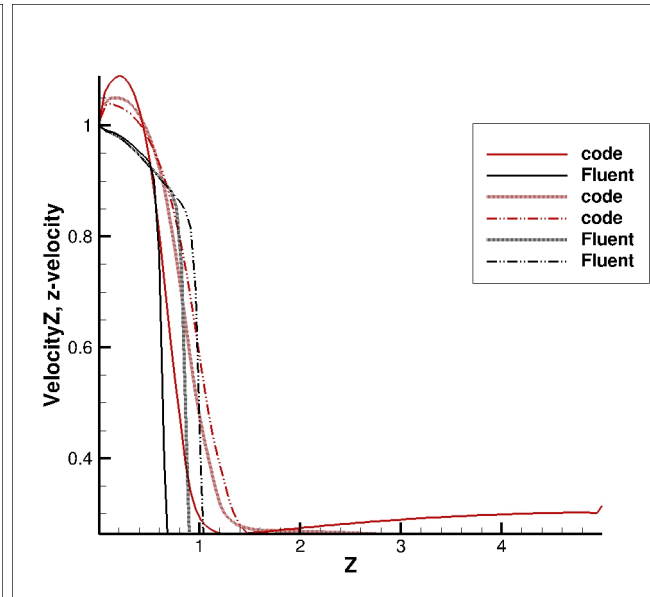


(d) $VF=0.4$

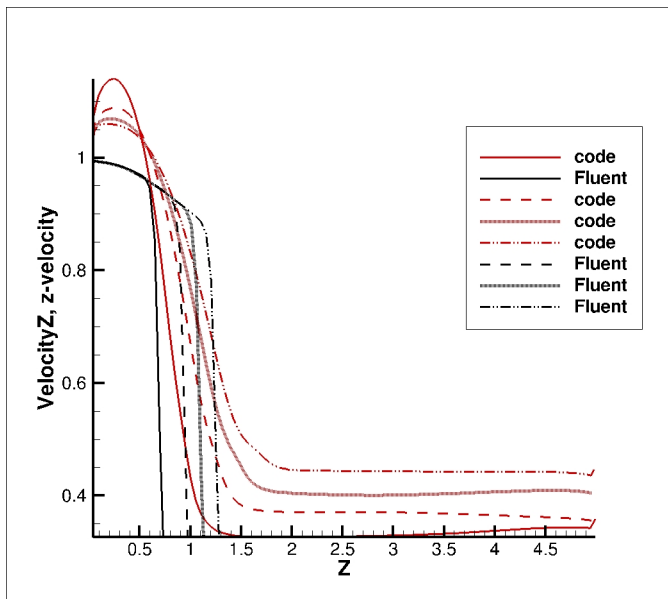
Figure 4.12: Comparison of Velocity Z for $Re = 500$ and $VF = 0.1, 0.2, 0.3, 0.4$ for density ratio 100



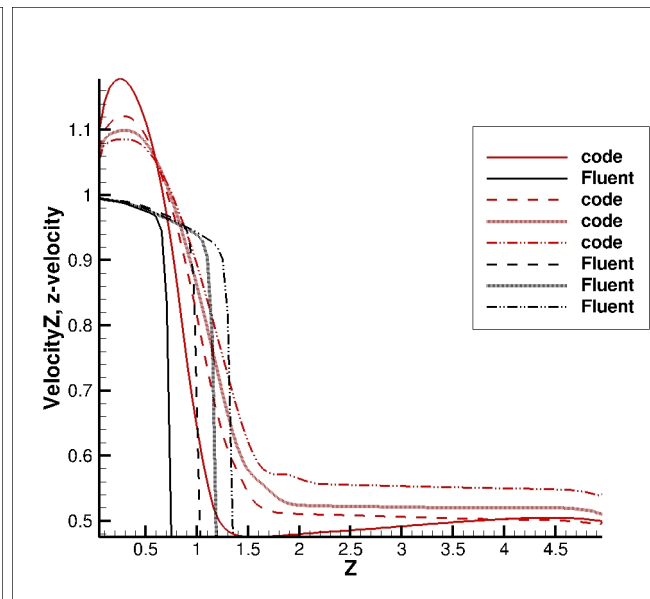
(a) $VF=0.1$



(b) $VF=0.2$



(c) $VF=0.3$



(d) $VF=0.4$

Figure 4.13: Comparison of Velocity Z for $Re = 1000$ and $VF = 0.1, 0.2, 0.3, 0.4$ for density ratio 100

Gravity

In many industrial applications, Jets are influenced by Gravitational field . Code is studied for density ratio 1.1, $Re = 100$, $VF = 0.1$ and $g = 9.8$, Gravity is applied in Z direction. From the figure 4.2.3 as time progresses difference in values of code and Fluent is increasing.

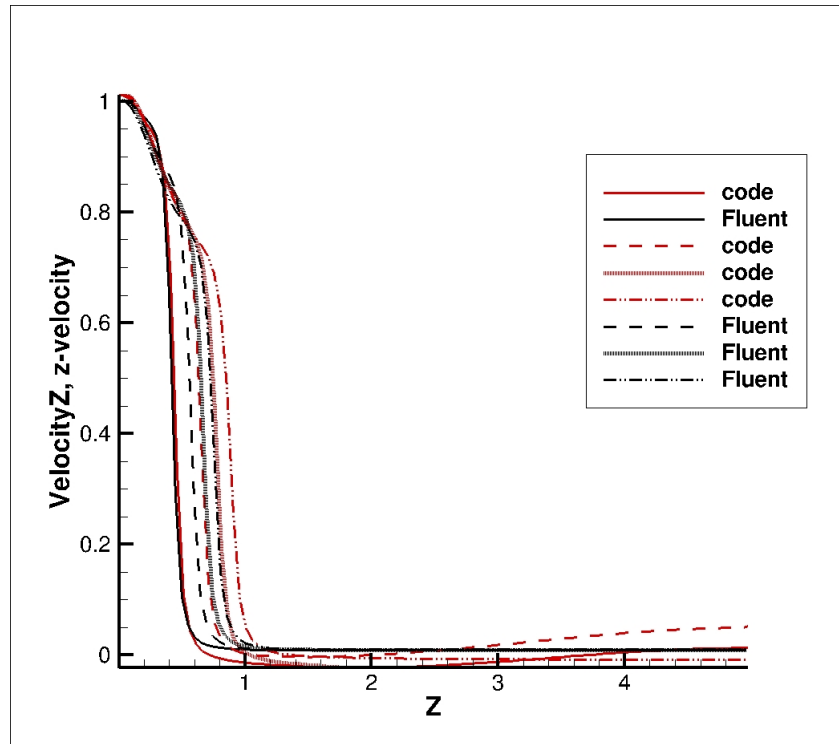


Figure 4.14: comparison of code and Fluent for gravity

4.3 Closure

From the above discussion, code is agreeing with Fluent for low density ratios with low volumetric loading. Over prediction is seen in code as time progresses. Code is unable to handle high density ratio and high volumetric loading.

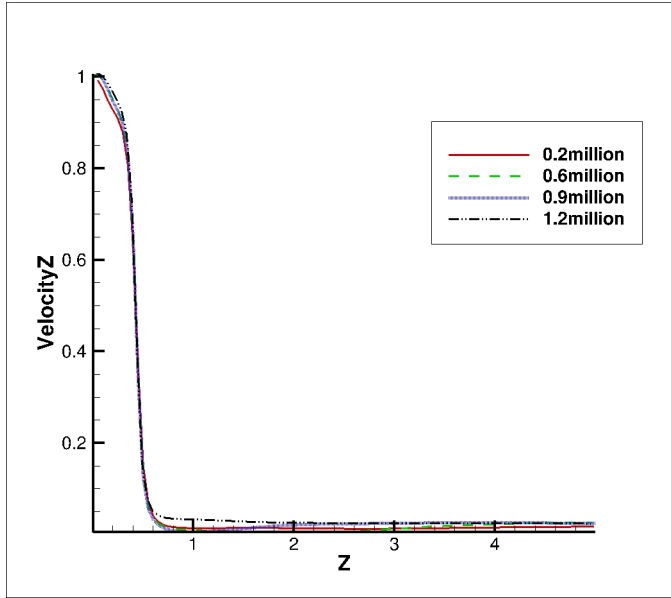
Chapter 5

Results and Discussion

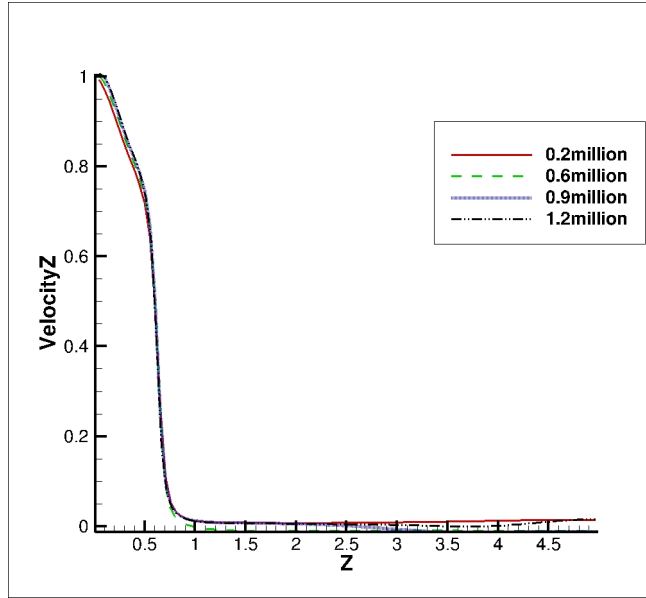
The Mesh dependency of the code is checked and different drag models are analyzed with varying Reynolds number and volumetric loading. In all the cases viscosity ratio (secondary phase to primary phase) is 1 and particle size taken to be $70\mu m$. Boundary conditions are given as mentioned in Chapter 4.

5.1 Grid Independence

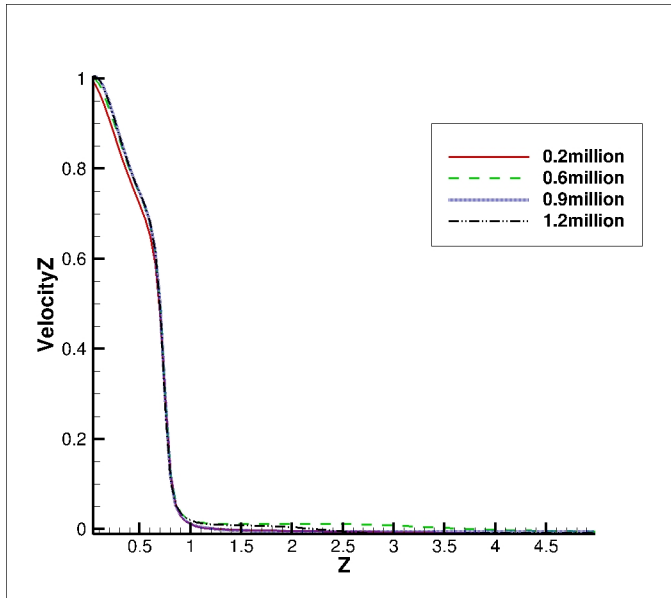
The Code is analyzed with different mesh sizes 0.2, 0.6, 0.9, 1.2 million. Comparison is done for 100 and 500 Reynolds number, with 0.1, 0.2 volumetric loading. From figures 5.1, 5.2, 5.3, 5.4, observed that for $Re = 100$ velocity profile is same for all the mesh sizes but as Reynolds number increased to 500 it showing small difference in values.



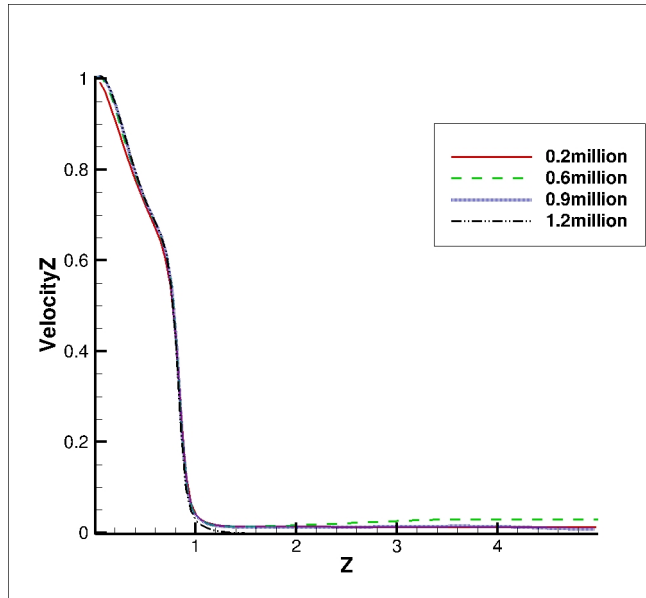
(a) time 1.0 sec



(b) time 1.5 sec

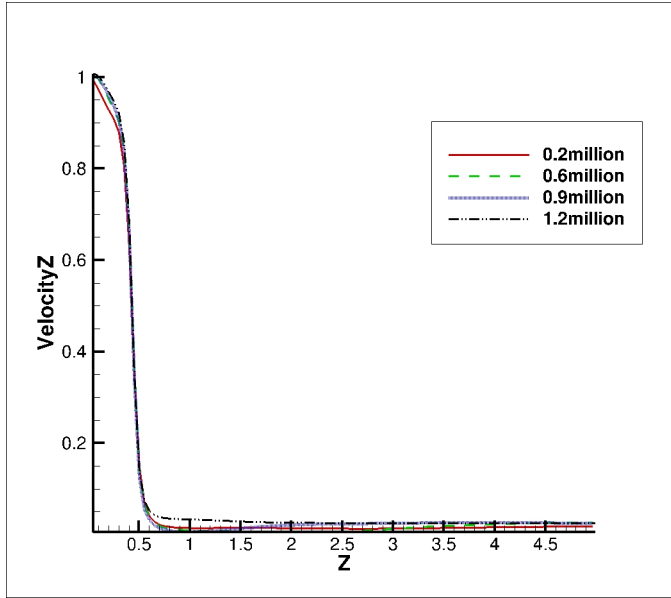


(c) time 2.0 sec

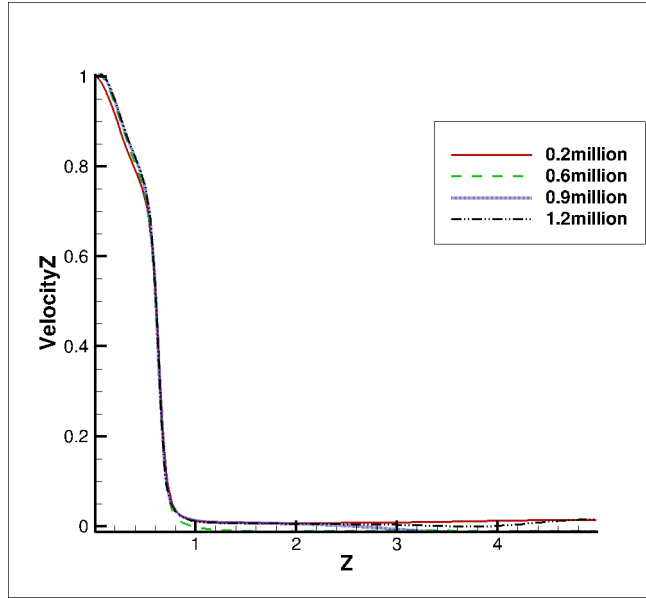


(d) time 2.4 sec

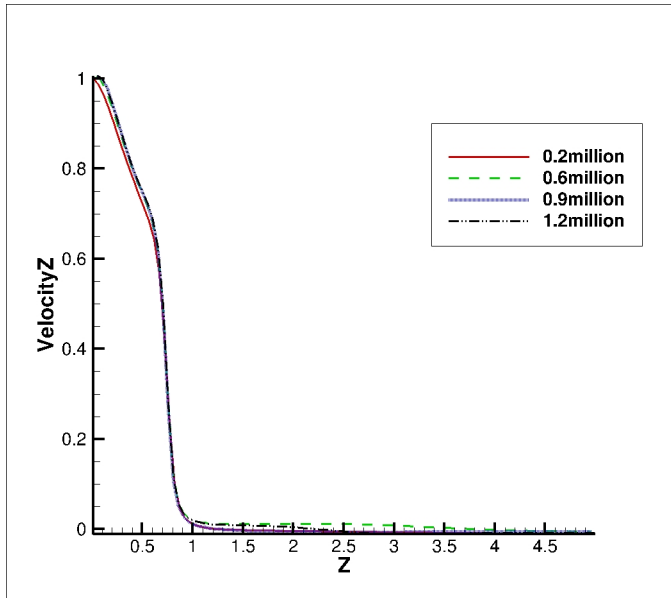
Figure 5.1: comparison at different time steps for $Re = 100$ with volume fraction at inlet $VF = 0.1$



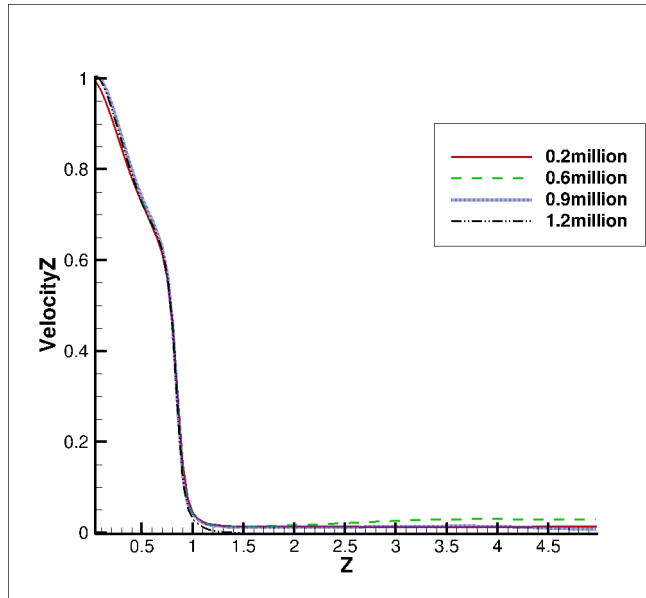
(a) time 1.0 sec



(b) time 1.5 sec

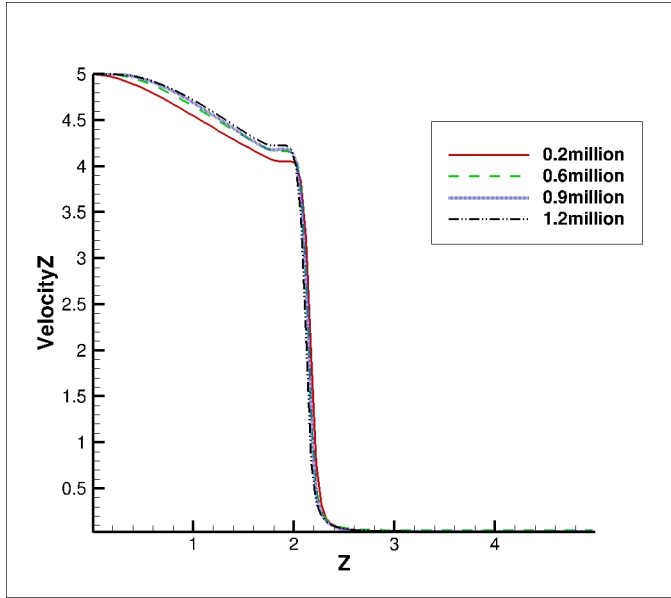


(c) time 2.0 sec

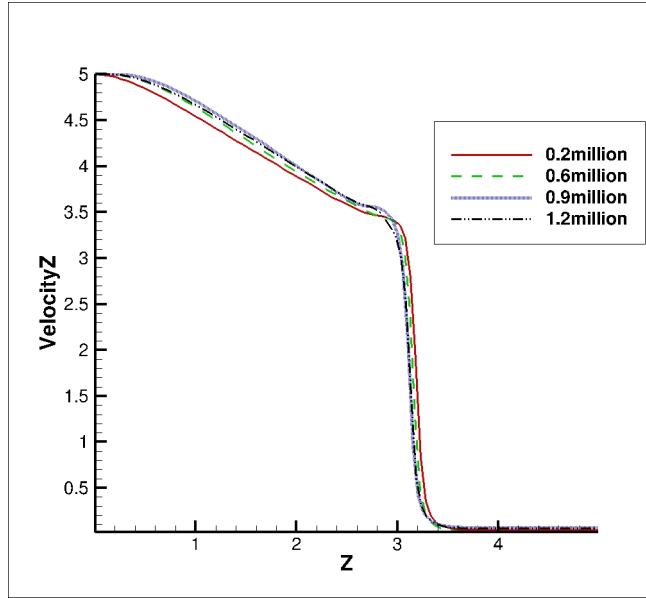


(d) time 2.4 sec

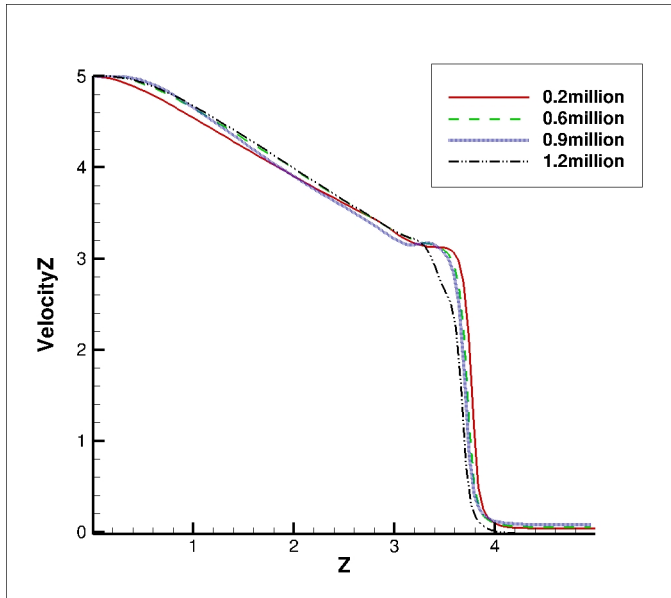
Figure 5.2: comparison at different time steps for $Re = 100$ with volume fraction at inlet $VF = 0.2$



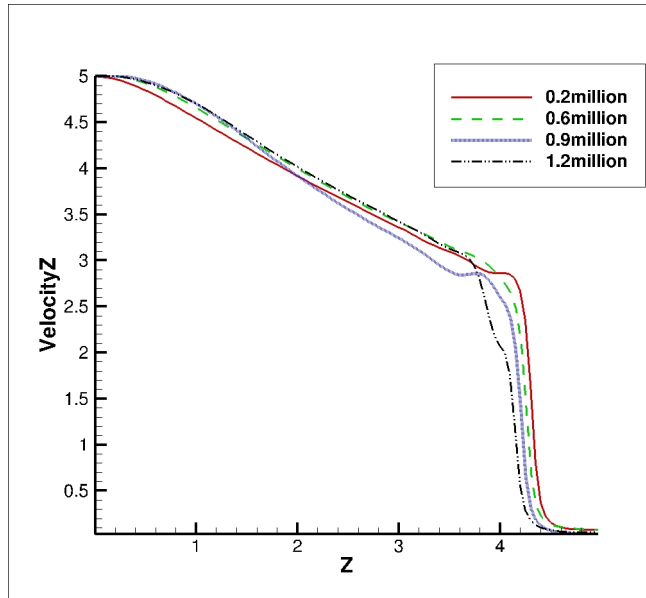
(a) time 1.0 sec



(b) time 1.5 sec

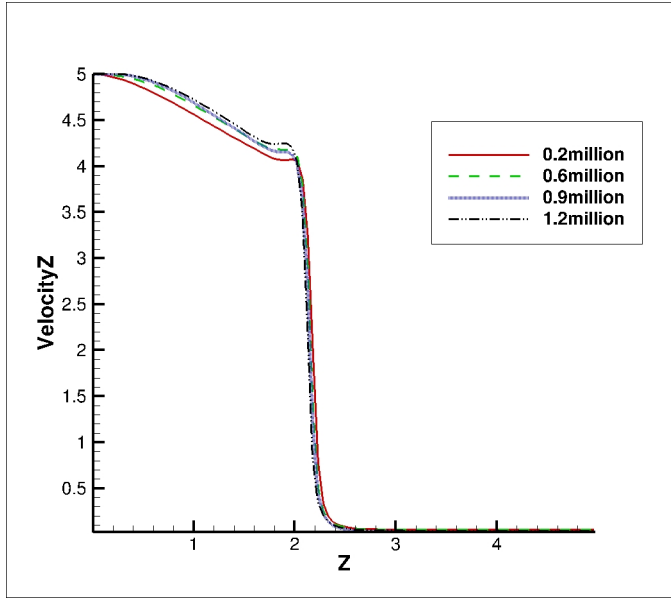


(c) time 2.0 sec

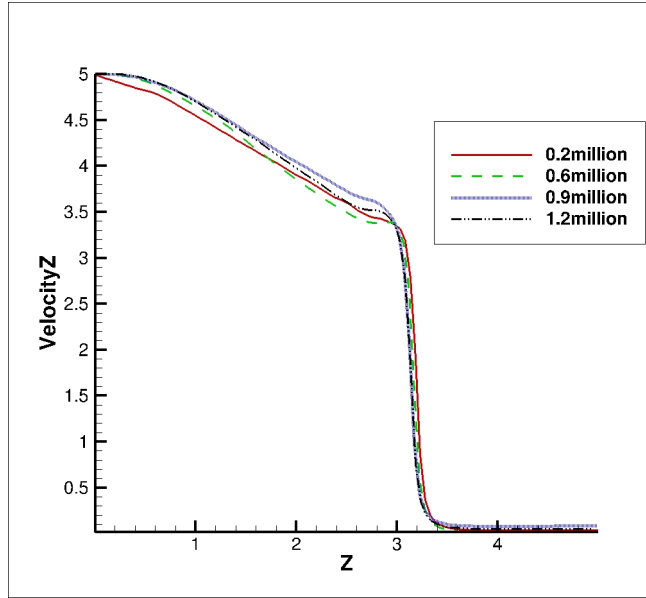


(d) time 2.4 sec

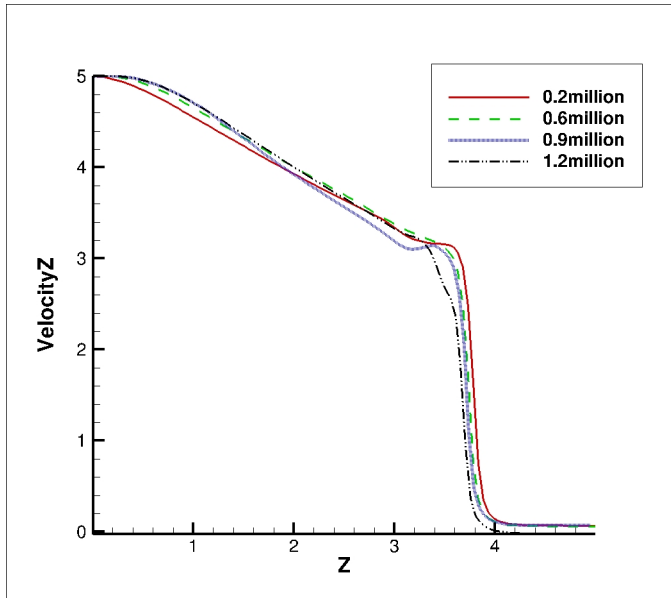
Figure 5.3: comparison at different time steps for $Re = 500$ with volume fraction at inlet $VF = 0.1$



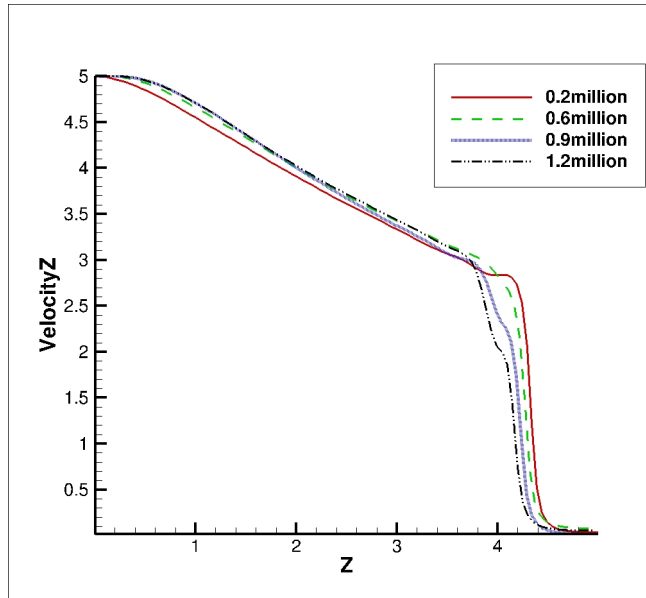
(a) time 1.0 sec



(b) time 1.5 sec



(c) time 2.0 sec

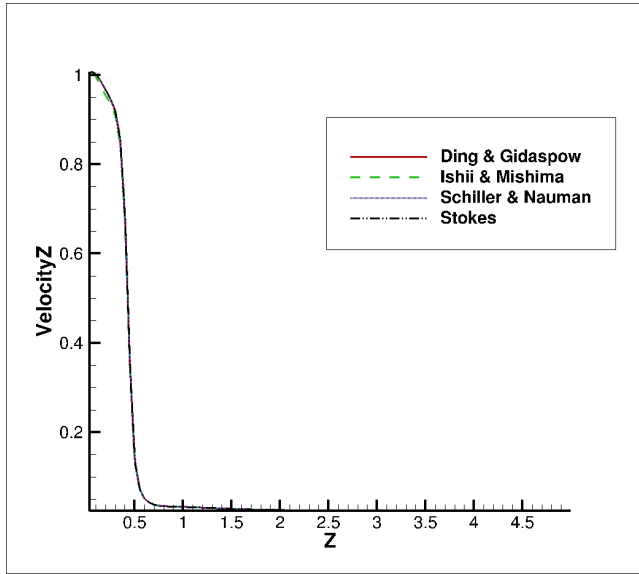


(d) time 2.4 sec

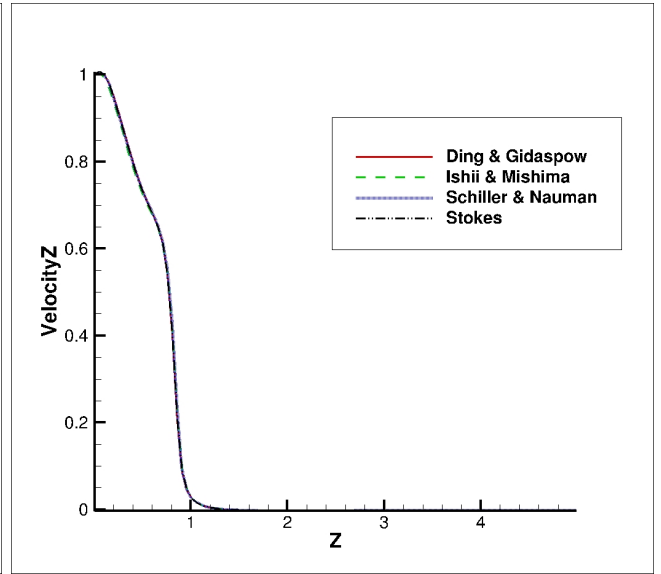
Figure 5.4: comparison at different time steps for $Re = 500$ with volume fraction at inlet $VF = 0.2$

5.2 Comparison of different Drag models

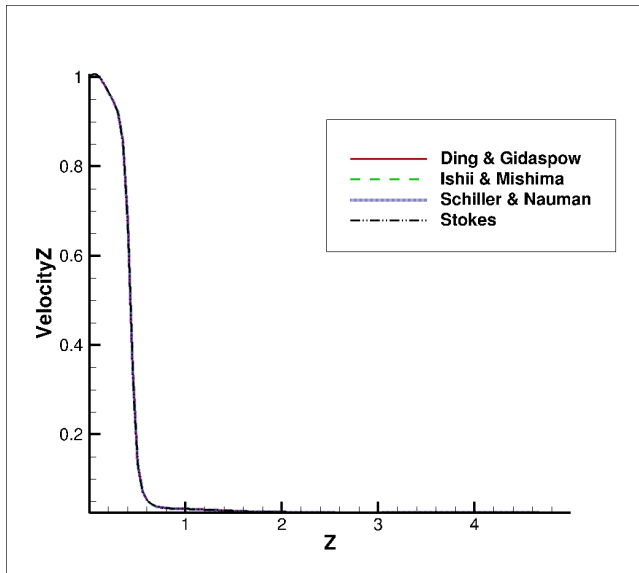
Different Drag models are implemented and analyzed with the code. The Models are Stokes (2.35), Schiller & Nauman (2.38), Ishii & Mishima (2.39), Ding & Gidaspow (2.40). The formulations are explained in Chapter 2. All of them compared for different Reynolds number 100 to 500 with 0.1, 0.2, 0.3 volumetric loading. From the figure 5.7,5.7,5.7,5.7 it is observed that there is no much difference in flow solution for different drag models. As flow is laminar and value of Reynolds number of particle is very low ($Re_p = \frac{d_p \rho_c |\mathbf{u}_{Cd}|}{\mu_c}$). Mikko Manninen & Veikko Taivassalo [3] have analyzed the drag function f_{drag} and drag coefficient C_D with different drag model. According to the report, there is no much difference in f_{drag} and C_D for low Re_p with low volumetric loading.



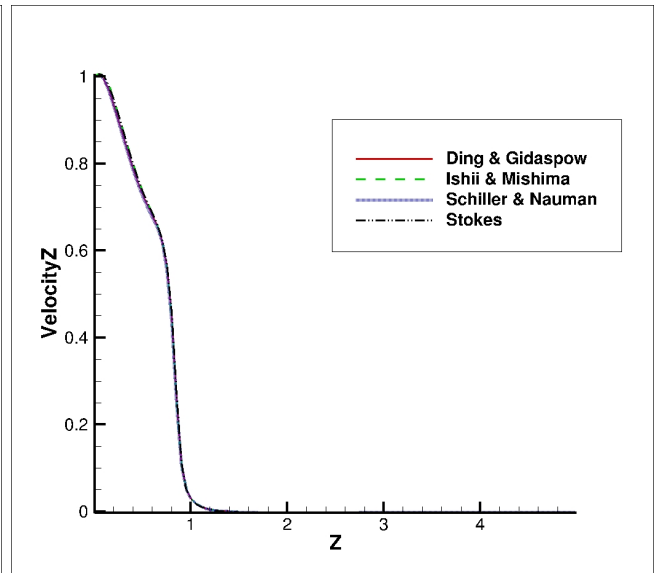
(a) $VF = 0.1, \text{time } 1.0 \text{ sec}$



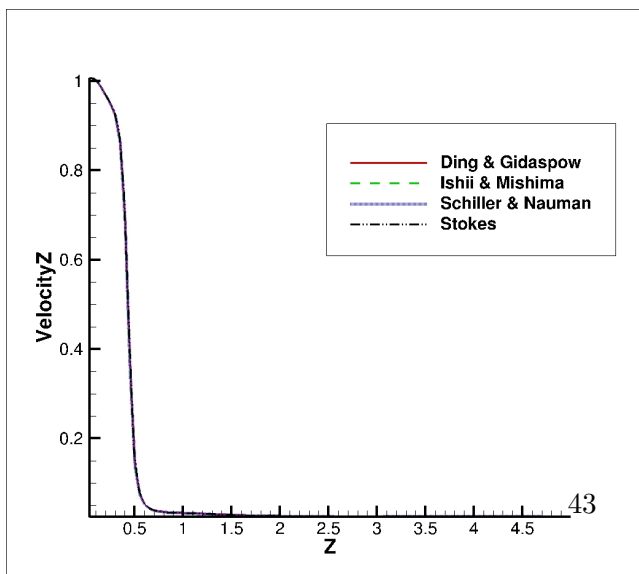
(b) $VF = 0.1, \text{time } 2.4 \text{ sec}$



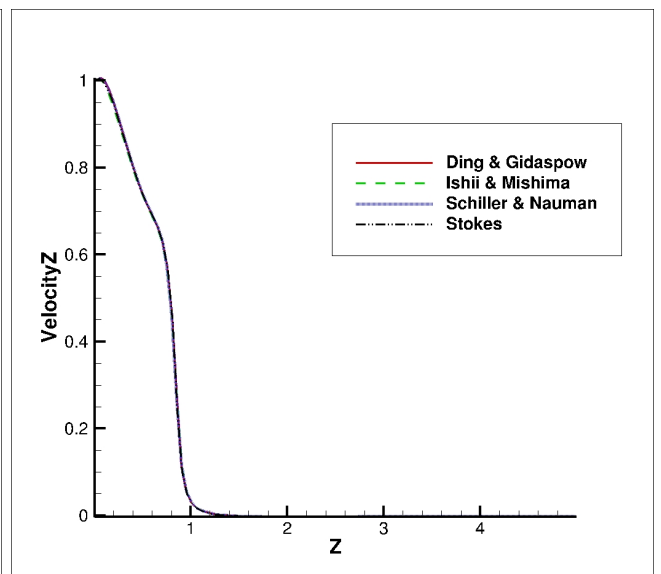
(c) $VF = 0.2, \text{time } 1.0 \text{ sec}$



(d) $VF = 0.2, \text{time } 2.4 \text{ sec}$

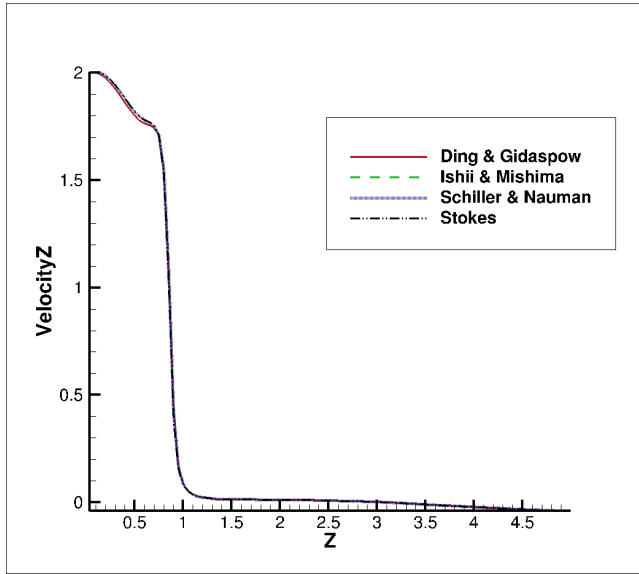


(e) $VF = 0.3, \text{time } 1.0 \text{ sec}$

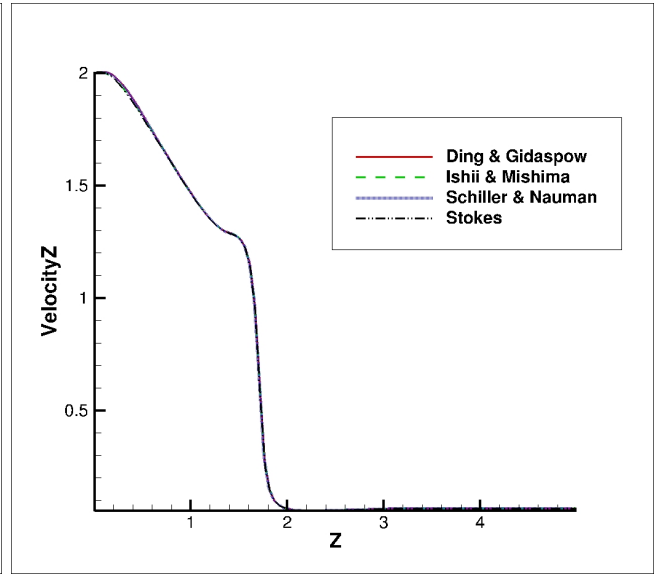


(f) $VF = 0.3, \text{time } 2.4 \text{ sec}$

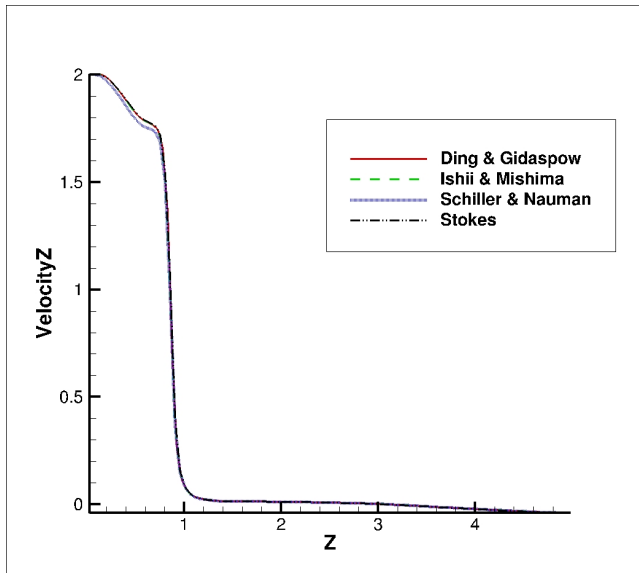
Figure 5.5: comparison at different time steps with different loading, different drag models for $Re = 100$



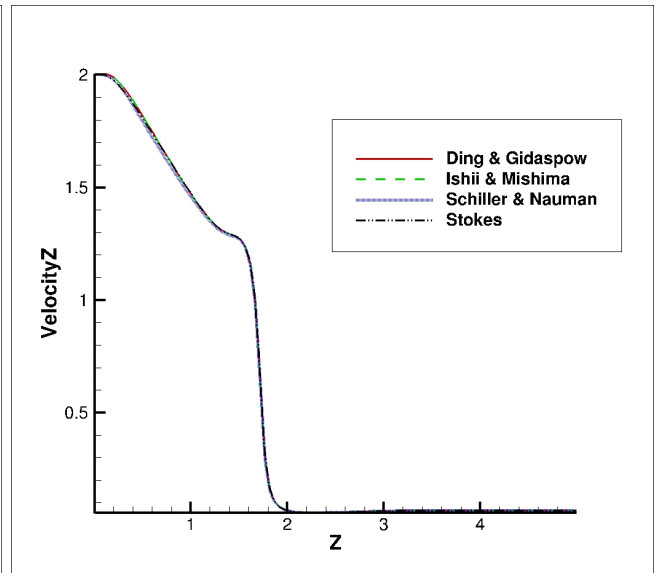
(a) $VF = 0.1$, time 1.0 sec



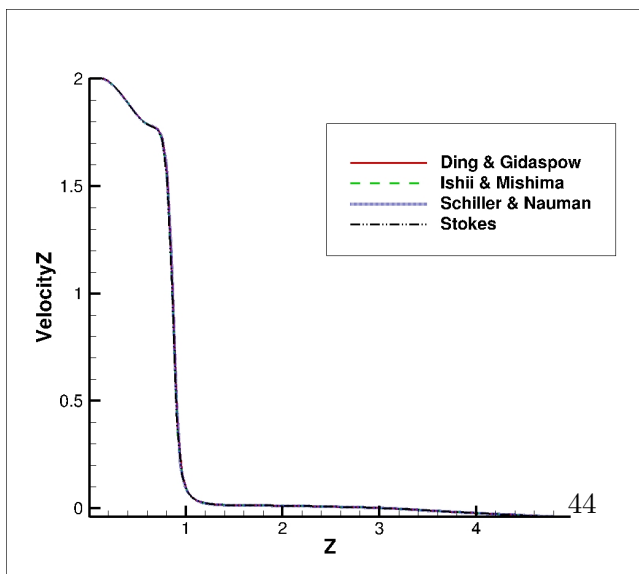
(b) $VF = 0.1$, time 2.4 sec



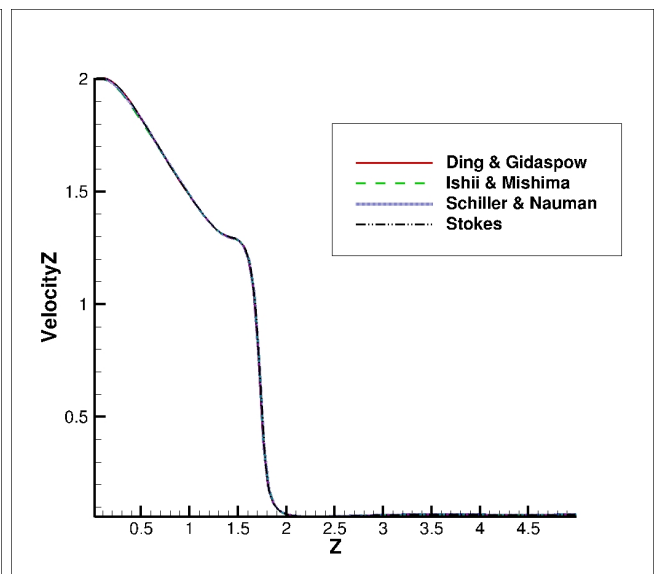
(c) $VF = 0.2$, time 1.0 sec



(d) $VF = 0.2$, time 2.4 sec

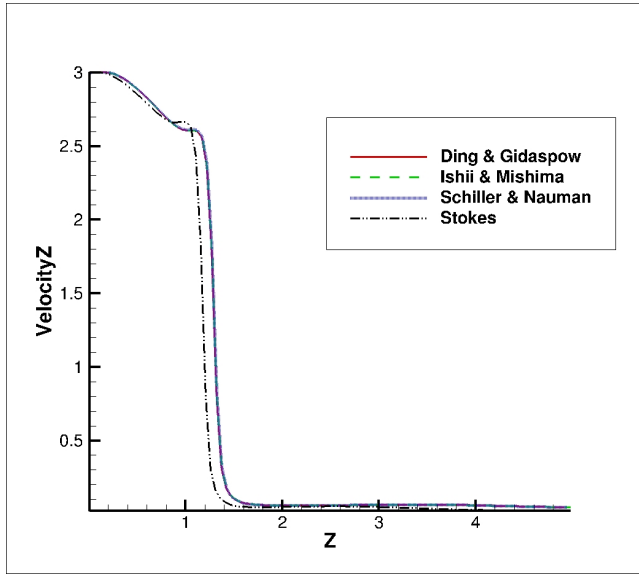


(e) $VF = 0.3$, time 1.0 sec

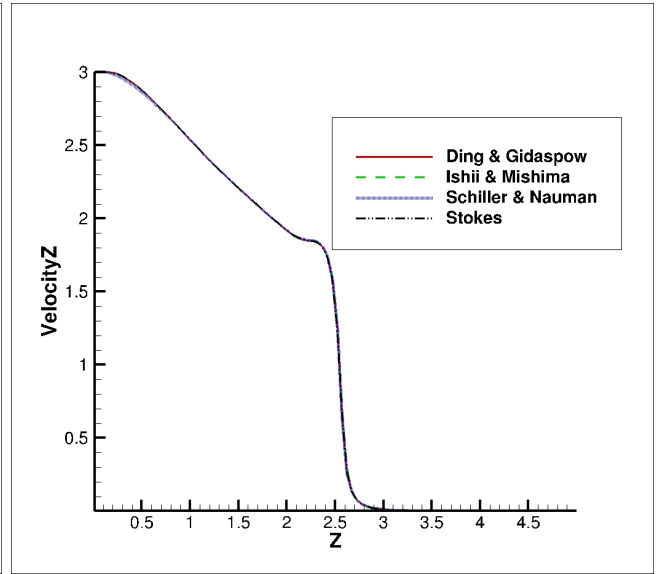


(f) $VF = 0.3$, time 2.4 sec

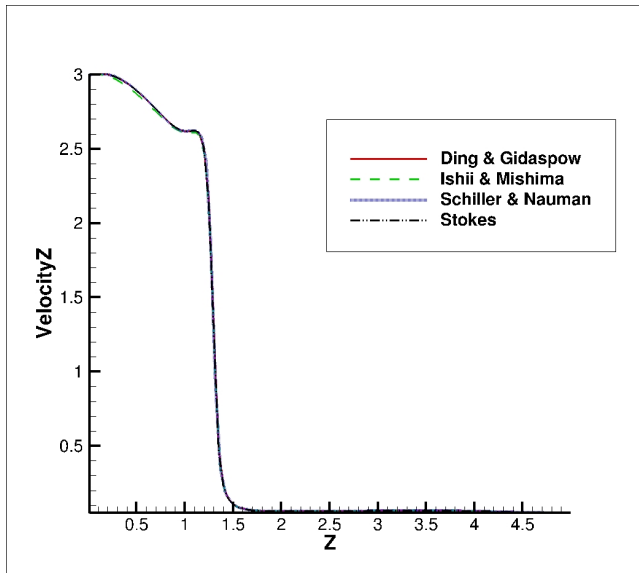
Figure 5.6: comparison at different time steps with different loading, different drag models for $Re = 200$



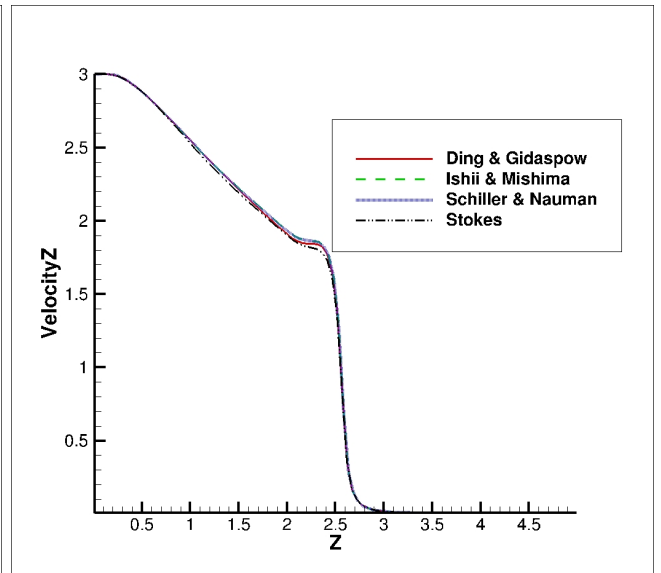
(a) $VF = 0.1$, time 1.0 sec



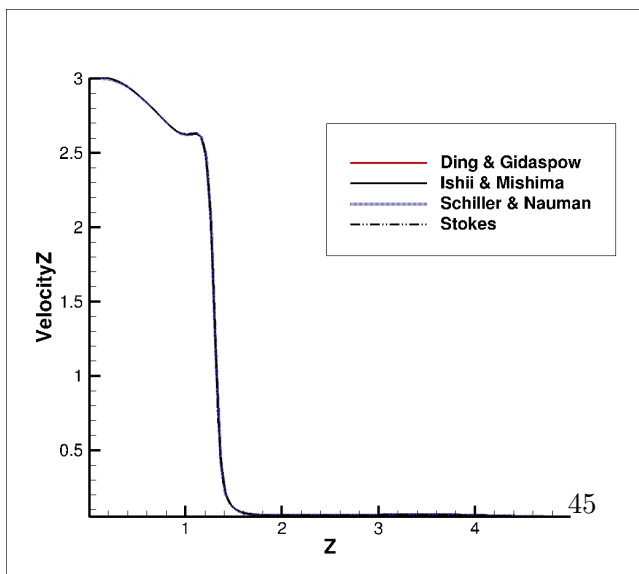
(b) $VF = 0.1$, time 2.4 sec



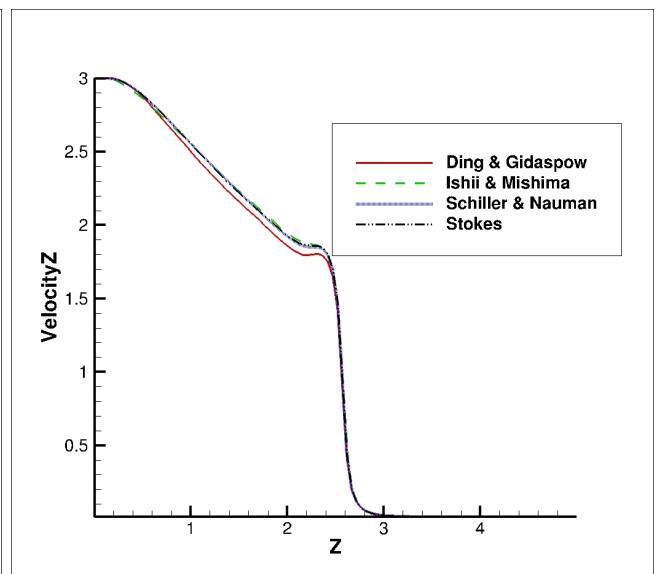
(c) $VF = 0.2$, time 1.0 sec



(d) $VF = 0.2$, time 2.4 sec

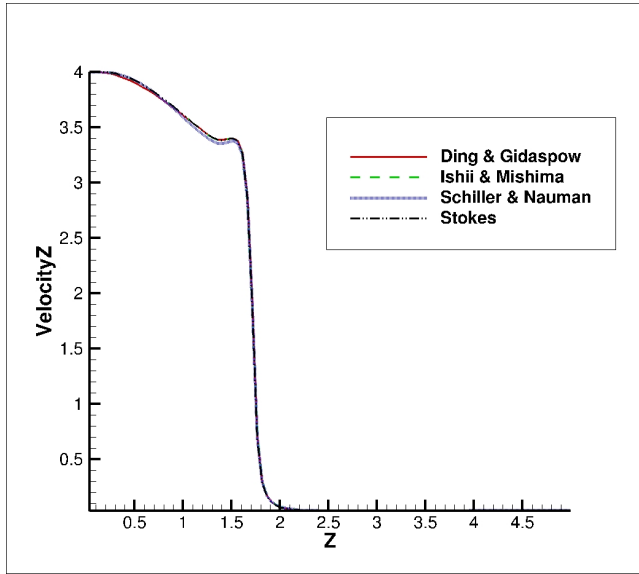


(e) $VF = 0.3$, time 1.0 sec

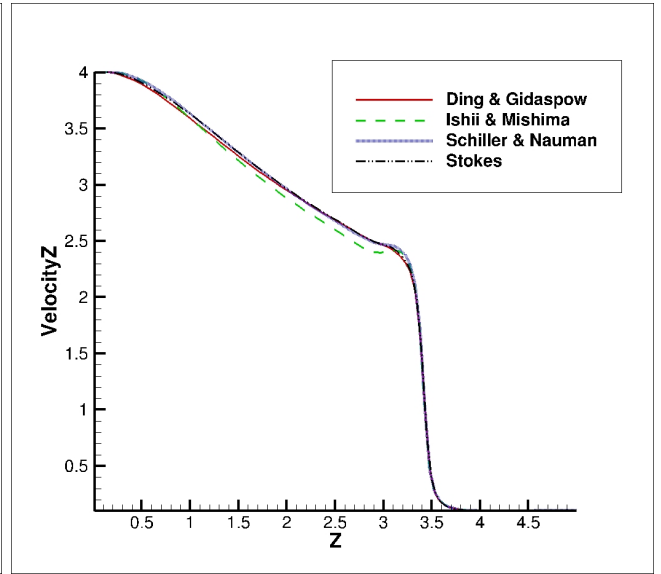


(f) $VF = 0.3$, time 2.4 sec

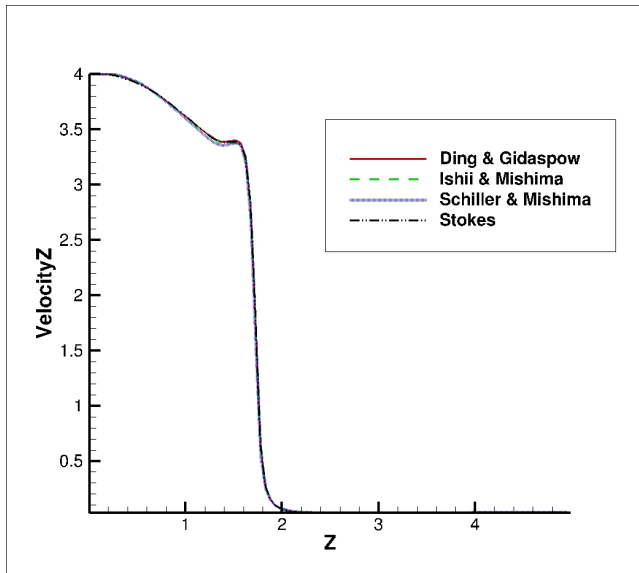
Figure 5.7: comparison at different time steps with different loading, different drag models for $Re = 300$



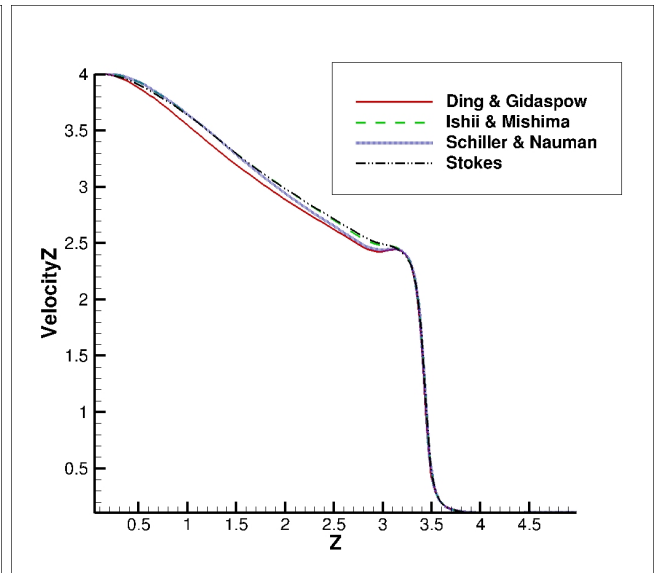
(a) $VF = 0.1$, time 1.0 sec



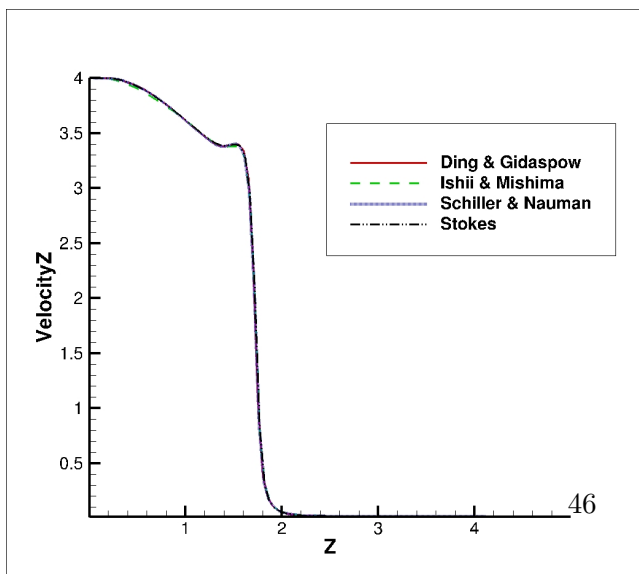
(b) $VF = 0.1$, time 2.4 sec



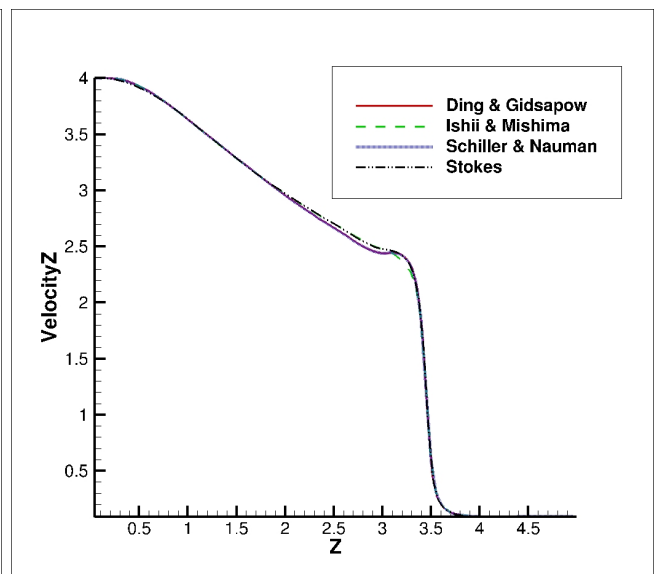
(c) $VF = 0.2$, time 1.0 sec



(d) $VF = 0.2$, time 2.4 sec

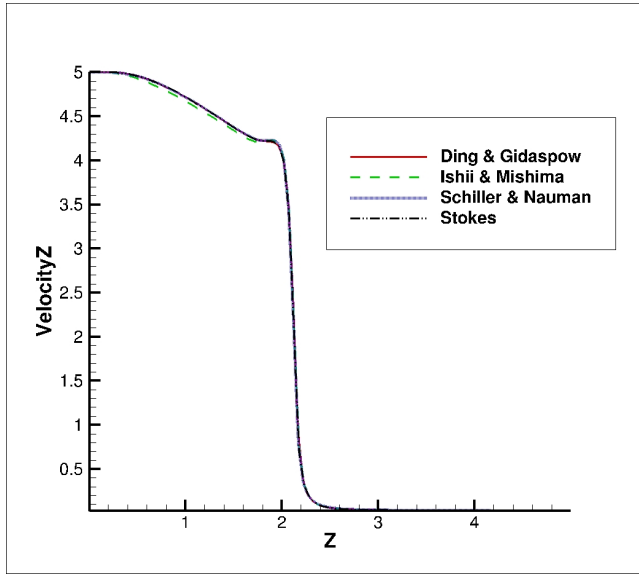


(e) $VF = 0.3$, time 1.0 sec

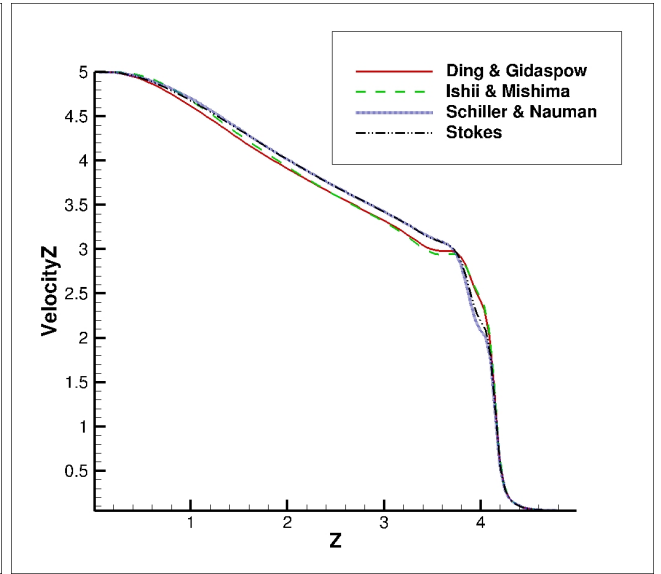


(f) $VF = 0.3$, time 2.4 sec

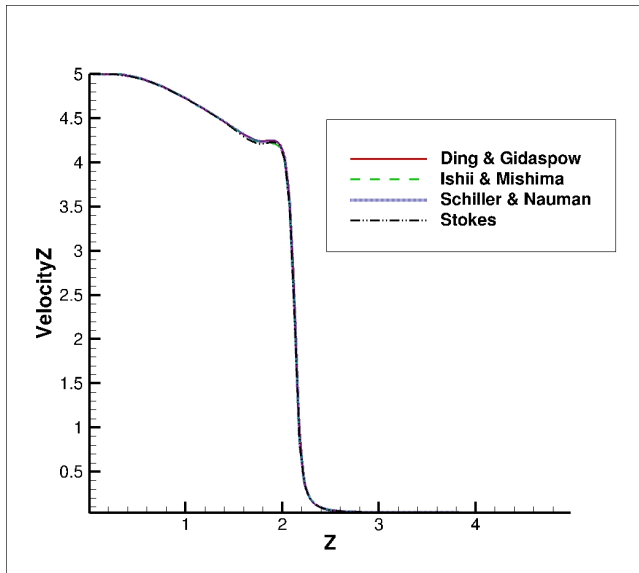
Figure 5.8: comparison at different time steps with different loading, different drag models for $Re = 400$



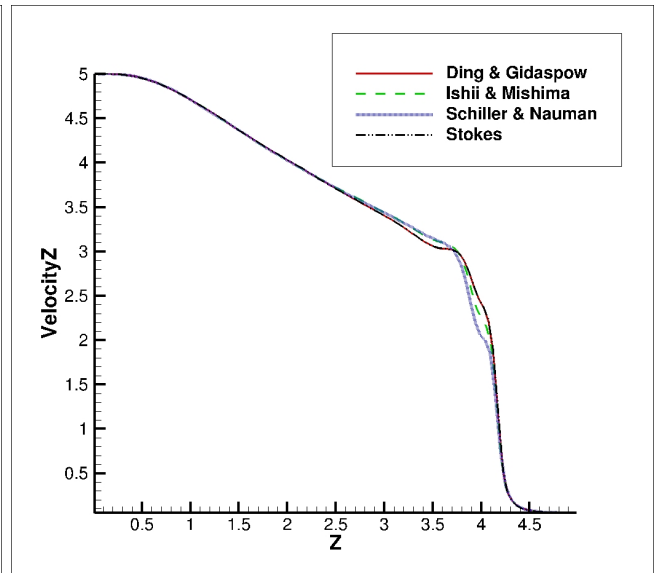
(a) $VF = 0.1$, time 1.0 sec



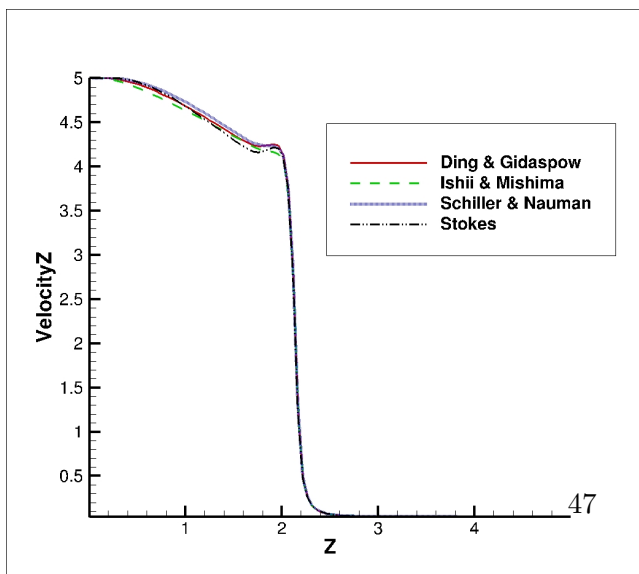
(b) $VF = 0.1$, time 2.4 sec



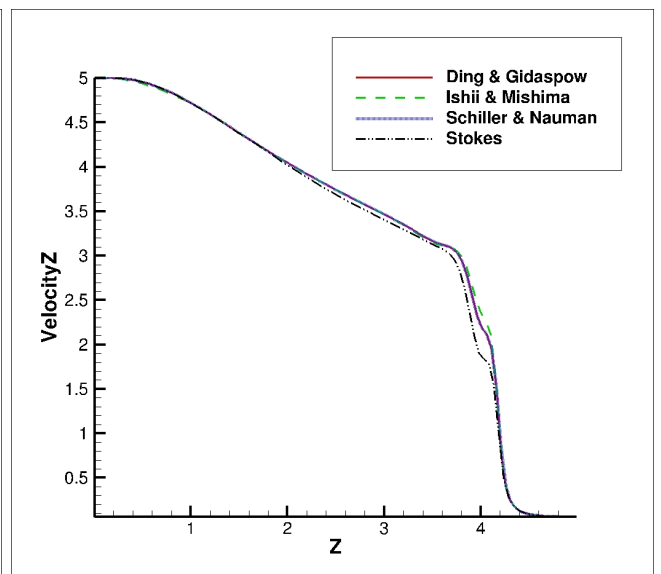
(c) $VF = 0.2$, time 1.0 sec



(d) $VF = 0.2$, time 2.4 sec



(e) $VF = 0.3$, time 1.0 sec



(f) $VF = 0.3$, time 2.4 sec

Figure 5.9: comparison at different time steps with different loading, different drag models for $Re = 500$

Shear Deformation

Due to the relative velocity between two phases, a shear deformation is observed on the Jet. When a Jet comes out from inlet it displaces existing phase and try to penetrate. Due to this vortices are formed on either side of the Jet. The figure 5.10 shows the following phenomenon.

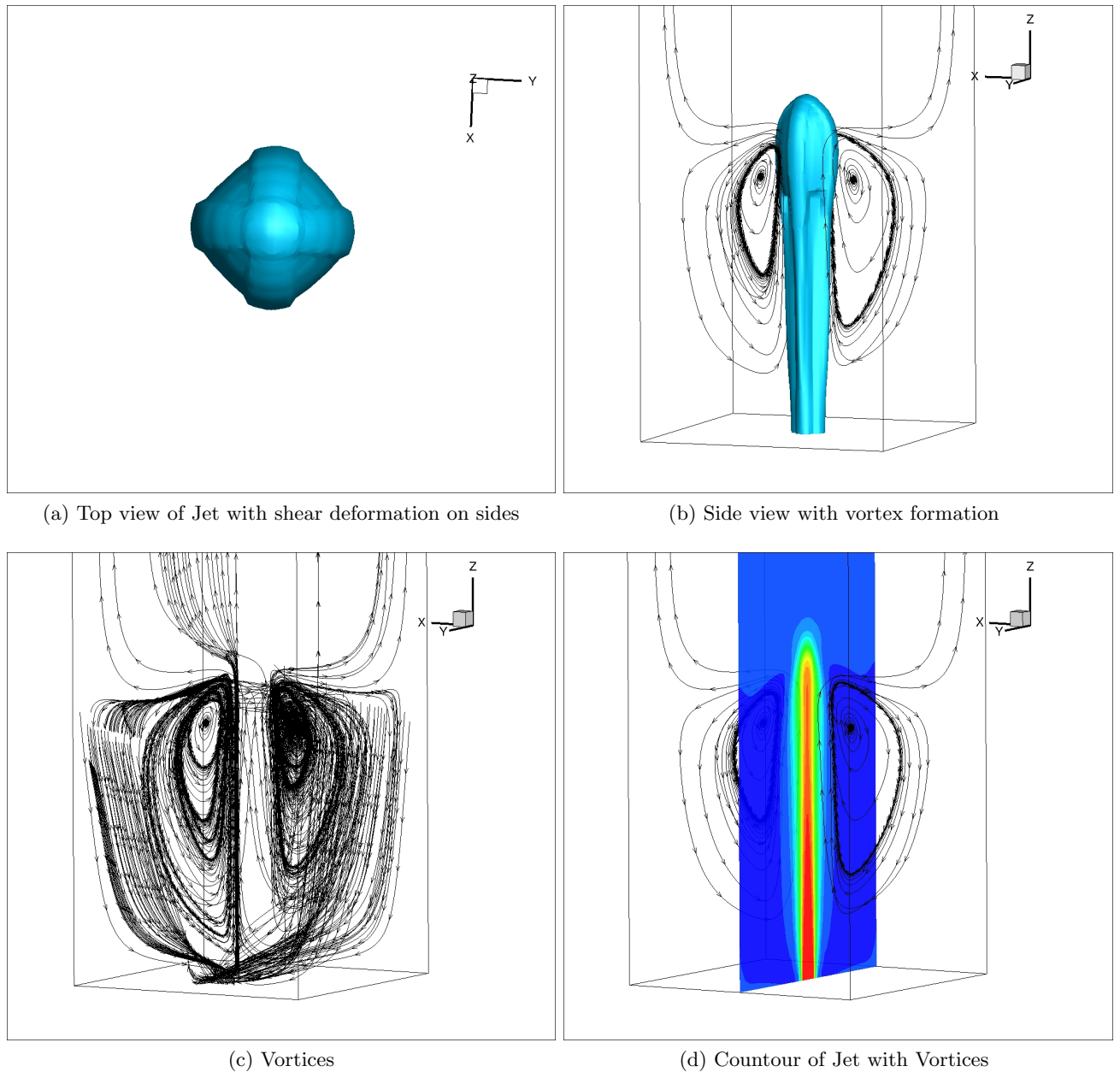


Figure 5.10:

Chapter 6

Conclusion and Future work

Building on the earlier work of Vatsalya Sharma[2], Multiphase module have been added to existing Single phase solver. A Lagrangian Algebraic Slip Mixture Model has been implemented and throughly validated for laminar cases. Validation is carried for Jet problems and compared with Fluent. It is observed that the solver results are same as Fluent for low density ratios with low volumetric loading. Over prediction of solution is observed in solver as time progresses. It may be rectified by switching to higher order convective schemes . For high density ratios, better interpolation scheme is required for calculation of density (ρ_m) terms at the faces.

Solver is checked for grid dependency. It is observed that for low Reynolds number solver is grid independent but as increase in Reynolds number causes difference in velocity profile between coarse and fine mesh. Different drag models are analyzed for various volumetric loading and Reynolds number. It is observed that for low volumetric loading and low particle Reynolds number (Re_d) all the models gives the same velocity profile. According to Mikko Manninen & Veikko Taivassalo [3], variation above parameters is observed at higher Re_d .

At the end, we are presenting a Multiphase solver with Lagrangian algebraic slip mixture model catering for industrial applications exclusively for Jets.

Following points can be used for future work.

1. Turbulence model LES is implemented but solver should be accelerated with LIS (Linear iterative solver) and AMG (Algebraic multi grid) techniques to get faster convergence.
2. Solver can be extended for more than two phases. To solve non-isothermal cases Scalar equation for energy has to be added .
3. Accuracy of Mixture model can be improved by adding forces like Lift force, Dispersion force, Virtual force in particle momentum equation.

Appendices

Appendix A

Source Terms Formulation

The discretization of Momentum , scalar and pressure poison equations according to the unstructured grid is explained in the thesis of Vatsalya Sharma [2]. The extra terms that are generated due to the derivation of Mixture model equations(2.58)(2.59) have to be discretized. By applying the control volume formulation the RHS term of Momentum equation may take the following form,

$$\int_V -\nabla \cdot \left[\rho_m C_d (1 - C_d) \mathbf{u}_{Cd} \mathbf{u}_{Cd} \right] = - \sum_f F_{Rel,f} \mathbf{u}_{cd,f} \quad (\text{A.1})$$

where subscript d is for disperse phase. And the flux is modeled as follows

$$F_{Relf} = \rho_{m,f} C_{df} (1 - C_{df}) [u_{cd,f} \cdot S_{fx} + v_{cd,f} \cdot S_{fy} + w_{cd,f} \cdot S_{fz}] \quad (\text{A.2})$$

From equation (2.21) C_d is written as

$$C_d = \frac{\phi_d \rho_d}{\rho_m} \quad (\text{A.3})$$

The quantities that have subscript f in (A.2) have to be calculated by volume interpolation formula.

$$u_{cd,f} = \frac{V_p u_{cd,n} + V_n u_{cd,p}}{V_n + V_p} \quad (\text{A.4})$$

here V denotes volume of the cell, subscript p denotes the current cell and n denotes the neighbor cell. The above volume interpolation is done for $v_{cd,f}, w_{cd,f}$, $\rho_{m,f}$ and C_{df} .

By applying Control volume formulation the RHS term of volume fraction equation may take the following form

$$\int_V -\nabla \cdot \left[\phi_d (1 - C_d) \mathbf{u}_{Cd} \right] = - \sum_f F_{vol,f} \phi_d \quad (\text{A.5})$$

the flux term is

$$F_{vol,f} = (1 - C_{df}) \left[u_{cd,f} \cdot S_{fx} + v_{cd,f} \cdot S_{fy} + w_{cdf} \cdot S_{fz} \right] \quad (\text{A.6})$$

The face values are determined as mentioned in equation (A.4).

References

- [1] Ishii,M. Thermo-fluid Dynamic Theory of Two-phase Flow. Paris:Eyrolles, 1975.
- [2] Vatsalya sharma. Development of Parallel CFD solver for Three Dimensional Unstructured Grid. Master’s thesis, Indian Institute of Technology, Hyderabad 2014.
- [3] Mikko Manninen,& Veikko Taivassalo. On the mixture model for multiphase flow. VTT Publications 288, Technical research center of Finland, 1996.
- [4] Zuber.N,& Findlay,J.A. Average Volumetric Concentration in Two-phase Flow systems. *Heat Transfer* 87, (1965) 453–468.
- [5] Pericleous,K.A. & Drake,S.N. An Algebraic slip model of PHOENICS for Multiphase applications. Numerical simulation of Fluid flow and Heat/Mass Transfer processes .
- [6] Verloop, W.C. The inertial coupling force. *Multiphase Flow* 21, (1995) 929–933.
- [7] Ungarish,M. Hydrodynamics of suspensions: Fundamentals of Centrifugal and gravity separation. Berlin:springer, 1993.
- [8] Johansen,S.T, Anderson,N.M, & De Silva,S.R. A Two-phase model for particle local equilibrium applied to air classification powder. *Powder Technology* 63, (1990) 121–132.
- [9] Drew, D.A. . Mathematical modeling of two-phase flows. *Fluid mechanics* 15, (1983) 261–291.
- [10] Drew, D.A. & Lahey,R.T. . Application of general constitutive principles to the derivation of multidimensional two-phase flow equations. *Multiphase flow* 5, (1979) 243–264.
- [11] Ishii. M. & Zuber, N. Drag coefficient and relative velocity in bubbly, droplet and particle flow. *AIChE* 25, (1979) 843–854.
- [12] Clift, R., Grace, J.R. & Weber, M.E. Bubbles, Drops and Particles. London: Academic press, 1978.
- [13] Ishii. M. & Mishima, K. Two-Fluid model and Hydrodynamic constitutive relations. *Nuclear Engineering* 82, (1984) 107–126.

- [14] Ding, J. & Gidaspow, D. A bubbling fluidization model using kinetic theory of granular flow. *AIChE* 36, (1990) 523–538.
- [15] O’Brien, T.J. & Syamlal, M. . Particle cluster effect in numerical simulation of a circular fluidized bed. *4th Int Conf on CFB* 430–435.
- [16] ungarish, M. & Amberg, G. Spin-up from rest of a mixture: numerical simulation and asymptotic theory. *Fluid mechanics* 246, (1993) 443–464.
- [17] Dahlkild, A.A. & Amberg, G. Rotating axial flow of a continuously separating mixture. *Fluid mechanics* 266, (1994) 319–346.
- [18] Brennan, M. CFD Simulations of Hydrocyclones with an Air Core: Comparison Between Large Eddy Simulations and a Second Moment Closure. *Chemical Engineering Research and Design* 84, (2006) 495–505.
- [19] M. Narasimhaa, M.S. Brennanb. A comprehensive CFD model of dense medium cyclone performance. *Minerals Engineering* 20, (2006) 414–426.
- [20] Z.Shang, J.Lou, H.Li . CFD of dilute gas-solid two-phase flow using Lagrangian algebraic slip mixture model. *Powder Technology* 266, (2014) 120–128.
- [21] Alhajraf, S. Computational fluid dynamic modeling of drifting particles at porous fences. *Environmental Modeling and Software* 19, (2004) 163–170.
- [22] Akbarinia, A. Investigating the diameter of solid particles effects on a laminar nanofluid flow in a curved tube using a two phase approach. *Heat and Fluid Flow* 30, (2009) 706–714.
- [23] Ruichang, Y., Rongchuan, Z., & Yanwu, W. The analysis of two dimensional two phase flow in horizontal heated tube bundles using drift flux model. *Heat and Mass Transfer* 35, (1999) 81–88.
- [24] Dalal, A., Eswaran, V. & Biswas, G. . A finite volume method for Navier stoke equations on unstructured meshes. *Numerical Heat Transfer* 54, (2008) 238–259.
- [25] Yonemura, S., Tanaka, T. & Tsuji, Y. Cluster formation in gas-solid flow predicted by the DSMC method, volume 166. 1993.
- [26] Gidaspow, D. Multiphase flow and fluidization. continuum and kinetic theory descriptions. San Diego: Academic press, 1994.
- [27] Simonin, O. Eulerian formulation for particle dispersion in turbulent two phase flow. *Workshop on Two Phase Flow Predictions* 156–166.
- [28] A.Guha. Transport and deposition of particles in Turbulent and Laminar flow. *Fluid mechanics* 40, (2008) 311–341.

- [29] Ungarish, M. On the modeling and investigation of polydispersed rotating suspensions. *Multiphase flow* 21, (1995) 267–284.